

Dwight Knox Library, NPS
Monterey, CA 93943

T211542

REPORT DOCUMENTATION PAGE		READ INSTRUCTIONS BEFORE COMPLETING FORM
1. REPORT NUMBER	2. GOVT ACCESSION NO.	3. RECIPIENT'S CATALOG NUMBER
4. TITLE (and Subtitle) MARINE SURFACE CONDENSER DESIGN USING VERTICLE TUBES WHICH ARE ENHANCED.		5. TYPE OF REPORT & PERIOD COVERED THESIS
7. AUTHOR(s) BARNES, CLIFFORD G. JR.		6. CONTRACT OR GRANT NUMBER(s)
8. PERFORMING ORGANIZATION NAME AND ADDRESS MASS. INST. OF TECHNOLOGY CAMBRIDGE, MA 02139		10. PROGRAM ELEMENT, PROJECT, TASK AREA & WORK UNIT NUMBERS
11. CONTROLLING OFFICE NAME AND ADDRESS CODE 031 NAVAL POSTGRADUATE SCHOOL MONTEREY, CA 93940		12. REPORT DATE JUN 81
14. MONITORING AGENCY NAME & ADDRESS (if different from Controlling Office)		13. NUMBER OF PAGES 125
16. DISTRIBUTION STATEMENT (of this Report)		15. SECURITY CLASS. (of this report) UNCLAS
17. DISTRIBUTION STATEMENT (of the abstract entered in Block 20, if different from Report)		18a. DECLASSIFICATION/DOWNGRADING SCHEDULE
18. SUPPLEMENTARY NOTES		
19. KEY WORDS (Continue on reverse side if necessary and identify by block number) MARINE CONDENSER DESIGN VERTICLE TUBE CONDENSERS ENHANCED TUBE CONDENSERS		
20. ABSTRACT (Continue on reverse side if necessary and identify by block number) ATTACHED		

ABSTRACT

A methodology is developed for calculating the heat transfer coefficient on the surface of a vertical fluted condenser tube based upon condensate film thickness. A marine condenser sizing procedure is demonstrated using this methodology. A comparison is made between a fluted tube condenser and a comparable smooth tube horizontal condenser. Alternative materials are considered and applicability is assessed for submarine use.

The results of the analysis indicate that a smaller volume, lighter weight condenser can be designed for marine use. The marine engineer can specify tube length or condensate drainage rate and size the condenser accordingly. Approximately 20% can be saved in volume, and, by using Titanium in place of Copper-Nickel, approximately 30% can be saved in tube bundle weight, compared to a similar horizontal condenser.

Approved for public release;
distribution unlimited.

MARINE SURFACE CONDENSER DESIGN USING
VERTICAL TUBES WHICH ARE ENHANCED

by

CLIFFORD GERALD BARNES, JR.
LIEUTENANT, US NAVY

B.S., United States Military Academy
(1974)

Submitted in Partial Fulfillment
of the Requirements of the Degrees of

OCEAN ENGINEER

and

MASTER OF SCIENCE IN MECHANICAL ENGINEERING

at the

MASSACHUSETTS INSTITUTE OF TECHNOLOGY

May 1981

© Clifford G. Barnes, Jr.

The author hereby grants to M.I.T. permission
to reproduce and to distribute copies of this
thesis document in whole or in part.

MARINE SURFACE CONDENSER DESIGN
USING VERTICAL TUBES
WHICH ARE ENHANCED

by

CLIFFORD GERALD BARNES, JR.
LIEUTENANT, U.S. NAVY

Submitted to the Department of Ocean Engineering
on 8 May 1981 in partial fulfillment of the
requirements of the Degrees of Ocean Engineer
and Master of Science in Mechanical Engineering.

ABSTRACT

A methodology is developed for calculating the heat transfer coefficient on the surface of a vertical fluted condenser tube based upon condensate film thickness. A marine condenser sizing procedure is demonstrated using this methodology. A comparison is made between a fluted tube condenser and a comparable smooth tube horizontal condenser. Alternative materials are considered and applicability is assessed for submarine use.

The results of the analysis indicate that a smaller volume, lighter weight condenser can be designed for marine use. The marine engineer can specify tube length or condensate drainage rate and size the condenser accordingly. Approximately 20% can be saved in volume, and, by using Titanium in place of Copper-Nickel, approximately 30% can be saved in tube bundle weight, compared to a similar horizontal condenser.

Thesis Supervisor: Warren M. Rohsenow
Title: Professor of Mechanical Engineering

To my brother, David

ACKNOWLEDGMENTS

The author wishes to express his appreciation to and respect for Professor Warren M. Rohsenow. Without his guidance and patience this thesis would still be an idea.

Thanks are due to CDR William Marsh, USN, Professor Paul Marto, Professor Kenneth Bell, and Dr. John Michele for collectively launching this effort with timely and seasoned advice.

A special measure of gratitude is reserved for the United States Navy, in which I proudly serve, for supporting my education and for never easing the pressure to succeed.

TABLE OF CONTENTS

	<u>Page</u>
ABSTRACT	2
ACKNOWLEDGEMENTS	4
TABLE OF CONTENTS	5
LIST OF FIGURES	7
LIST OF TABLES	8
CHAPTER I. INTRODUCTION	9
I.A. Background Information	9
I.B. Objectives of This Work	12
I.C. Design Inputs	17
CHAPTER II. TUBE SELECTION	22
II.A. Materials	22
II.B. Strength Requirements	29
CHAPTER III. ELEMENTS OF HEAT TRANSFER	33
III.A. Nomenclature	33
III.A. Heat Transfer Coefficient of Cooling Water	36
III.B. Heat Transfer Coefficient for a Tube Wall	37
III.C. Heat Transfer Coefficient for Condensation	38
III.D. Application to Condenser Design	55
III.E. Heat Transfer Resistance Due to Scaling	61
CHAPTER IV. DESIGN PROPOSALS	64
IV.A. Condenser Geometry	64
IV.B. Tube Attachment	66
CHAPTER V. RESULTS AND CONCLUSIONS	68
V.A. Comparison with Nusselt Analysis	68
V.B. Condenser Comparison Using Titanium	69
V.C. Conclusions	74
V.D. Recommendations	76
V.E. Summary	78
APPENDIX A. CONDENSER TUBE STRESS CALCULATIONS	79

	<u>Page</u>
APPENDIX B. CALCULATIONS FOR CONDENSATE FILM THICKNESS	89
APPENDIX B, ADDENDUM 1. Calculator Program for the solution of Equation (B.14b)	100
APPENDIX C. FLUTED CONDENSER SIZING PROCEDURE	110
REFERENCES. .	122

LIST OF FIGURES

		<u>Page</u>
I-1	Schematic showing condensation blockage effect on smooth horizontal and vertical tubes.	13
I-2	Fluted surface concept.	15
II-1	The effects of sea water velocity on corrosion resistance of various metals.	24
II-2	Behavior of titanium metal couples immersed in aerated sea water for 2500 hours.	30
III-1	Schematic showing fluted tube dimensions.	39
III-2	Coordinates for flute and condensate profile.	40
III-3	Schematic of fluid surface showing force balance between pressure and surface tension.	42
III-4	$Nu_O \Omega^{1/4}$ versus a/p	46
III-5	Nu/Nu_O versus w/w_f	48
III-6	Nu_O/Nu versus w/w_f	50
III-7a	M versus w/w_f , a/p = .15	51
III-7b	M versus w/w_f , a/p = .35	52
III-8	Schematic diagram showing stripper plate spacing and axial temperature distribution.	56
IV-1	A double-pass fluted condenser with six drainage segments.	65
IV-2	A proposed method for rolling fluted tubes into the tube sheet.	67
V-1	Nu_z/Nu_O versus w/w_f and M	70
A-1	Schematic of a condenser tube.	81
A-2	Load relieving factor, γ , as a function of flute geometry.	86

LIST OF TABLES

Page

I-1	Thermal conductivity and yield strength of several common metals and select alloys.	20
II-1	Mechanical properties and composition of marine condenser materials.	23
II-2	Galvanic series of metals in flowing sea water.	28
II-3	Tube specifications for various design depths. .	32
III-1	Sample calculations for condensate film thickness. .	43
III-2	Sample Calculations for $Nu_O \Omega^{1/4} = f(a/p)$	45
III-3	Calculated values for M and w/w_f for several different values of a/p	53
III-4	Sample results for a fluted condenser.	60
III-5	Values of F_{ox} , the resistance of the oxide film on the inside and outside surfaces of clean tubes	63
V-1	Comparison between condensers using Cu-Ni and Ti. .	71
V-2	Comparison between a horizontal and a fluted condenser.	75
C-1	Solution for L , with $(w/w_f)_1 = 0.060$	115
C-2	Solution for $(w/w_f)_2$ with $L_2 = 4.957$ ft.	117
C-3	Results for sizing the condenser as specified as appendix C.	118
C-4	Comparison between equation (III-22) and calculated results.	119

CHAPTER I

INTRODUCTION

A. Background Information

In the design of a marine power plant, overall thermal efficiency, weight, and volume are the driving concerns [1]. This is especially true for the steam plant, which is the predominant form of propulsion for large naval vessels. While a large marine diesel may provide better specific fuel consumption than a fossil fired steam plant, the latter retains several intrinsic characteristics which make it attractive for naval propulsion. These advantages include:

1. Use of alternative heat sources.

In the case of a submarine, aircraft carrier, or cruiser, a nuclear reactor provides the thermal energy. In smaller ships, a boiler is used as the steam generator.

2. Auxiliary steam generation.

Auxiliary steam provides water, hotel services, and drives auxiliary equipment such as steam catapults on an aircraft carrier.

3. High speed.

The steam plant has a much wider operating range than a large marine diesel. The design of a naval steam plant usually provides for

redundancy of steam generators which allows for much higher speeds than a comparable sized diesel plant.

4. Endurance.

The steam plant which has a nuclear reactor as its heat source requires neither air nor refueling during a specific mission.

There are advantages to other types of propulsion plants, but the brief list above points out that for certain applications the steam plant is irreplaceable. The high speed, large shaft horsepower, and endurance required by an aircraft carrier, and the covert endurance required by a submarine dictate the need for a steam propulsion system. In the aircraft carrier, thermal efficiency may be paramount to the design of the plant due to large demands by auxiliary systems, but in the submarine, weight and volume are critical.

In the submarine design, 25 percent of all the useful weight is devoted to propulsion. This term, for the sum of all useful weight, is "normally submerged condition," (NSC), and it is the submerged displacement minus the ballast water necessary to maintain neutral buoyancy [2]. The design process for the submarine is to first lay out the machinery section and determine its critical

length. This length is referred to as the "stack length." Once the stack length has been established along with its weight and volume, the remaining required weights are added, and the overall buoyant envelope can be determined [3]. This envelope is the volume necessary for neutral buoyancy. The stack length, therefore seriously impacts on the total volume of the submarine, and the weight of the machinery also becomes a constraint. With these two constraints merely removing weight from within the buoyant envelope, may be insufficient to allow the reduction of the envelope. Weight removal must often be countered with addition of lead ballast. Conversely, reducing the volume of the hull, but not the weight causes negative buoyancy. Also, the decrease in volume of specific items within the buoyant envelope allows greater freedom in arrangement, but unless accompanied by a commensurate weight reduction, a decrease in NSC will not be realized.

Consider the fact that a Los Angeles class attack submarine (SSN-688) costs 460 million FY-81 dollars [4]. This cost includes the cost of construction plus all government furnished equipment. The dimensions of this submarine are: length, 362 ft; diameter, 33 ft; and submerged displacement, 6900 tons [5]. A very crude

approximation would say that each foot of length costs one million dollars and displaces 19 tons. So a moderate reduction in the stack length which is accompanied by the appropriate weight reduction should be worth several million dollars in acquisition, with second order effects being felt in horsepower requirements.

B. Objectives of this Work

The objective of this thesis is to develop a design methodology for an alternative surface condenser than those presently used in marine steam plants. This alternative condenser is expected to be smaller and lighter than existing units, and it will have a higher overall heat transfer coefficient.

The average condensation heat transfer coefficient on a smooth surface horizontal tube steam condenser is approximately $2000 \text{ BTU/hr ft}^2 \text{ }^\circ\text{F}$. Condensation inundation of tubes which are lower in the condensing tube bundle significantly reduces their heat transfer effectiveness [6]. Vertical orientation of the smooth tube bundle would not solve this inundation problem because a developing boundary layer would cause similar adverse effects. Figure I-1 shows the blocking effect of the fluid for horizontal and vertical tubes.

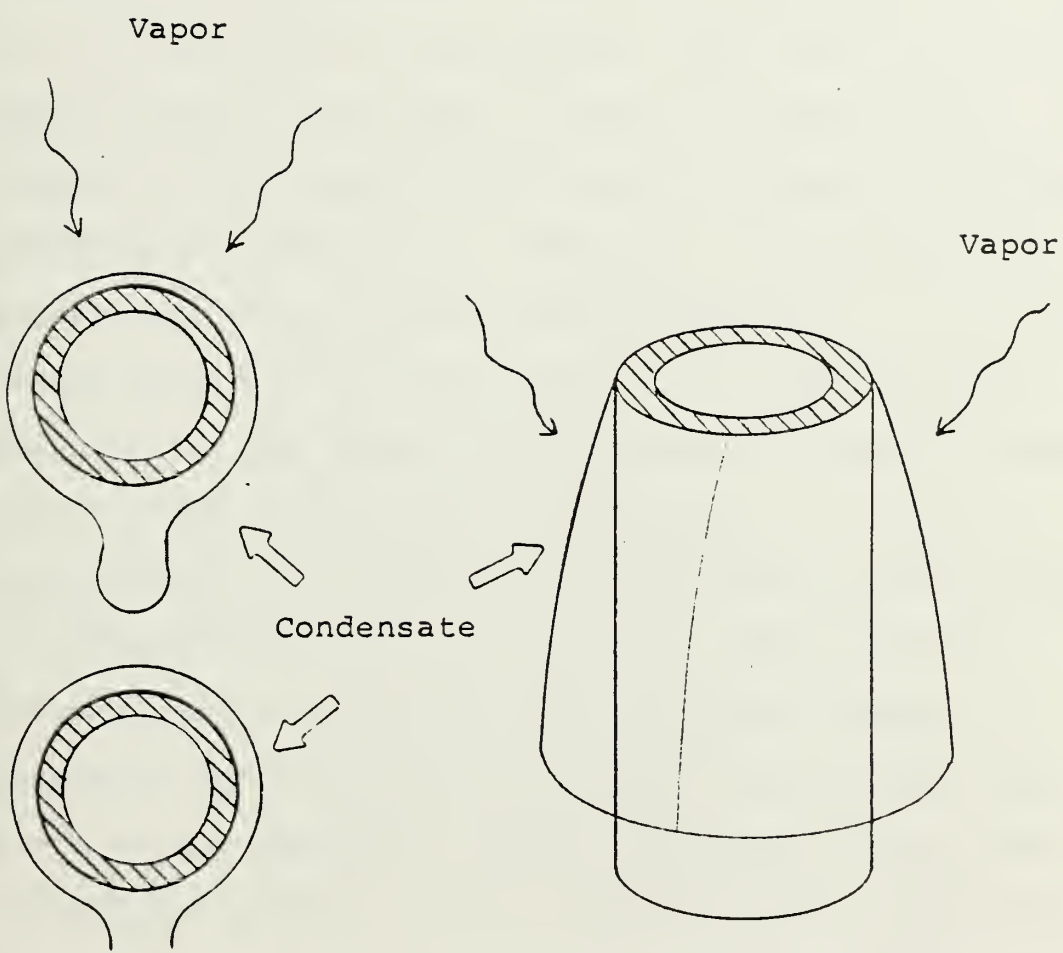


Figure I-1: Schematic showing condensation blockage effect on smooth horizontal and vertical tubes.

In 1954 Gregorig proposed condensing on vertically oriented tubes with fluted axial surfaces [7]. Surface tension of the condensate draws the liquid into the valleys of the flute where it then drains down, leaving a thinner liquid layer on the peaks. Figure I-2 demonstrates this concept. Heat transfer coefficients predicted for these condensing surfaces using Gregorig's fluid properties and temperature drops approach 8000 BTU/hr ft²°F. In a procedure developed by Zener and Lavi [8] and refined by Webb [9] for the design of an optimized Gregorig condensing surface, heat transfer coefficients as high as 36000 BTU/hr ft²°F are reported by experiment and as high as 55000 BTU/hr ft²°F are predicted. These surfaces, however, may be difficult to manufacture, and for a generally curved repeating surface of such small dimensions as are required, the exact geometry may not be a significant influence on the condensing heat transfer coefficient [10]. The extrusion capabilities of industry are likely to set the limits on the geometry of the flute, and for these reasons a quite regular geometry such as a sine flute is considered. Longitudinal machining or axial welding to achieve a specific surface geometry is not acceptable for condenser tubes which are used in naval vessels [11]. By requiring seamless drawn tubes for naval condensers, residual stresses and machining flaws

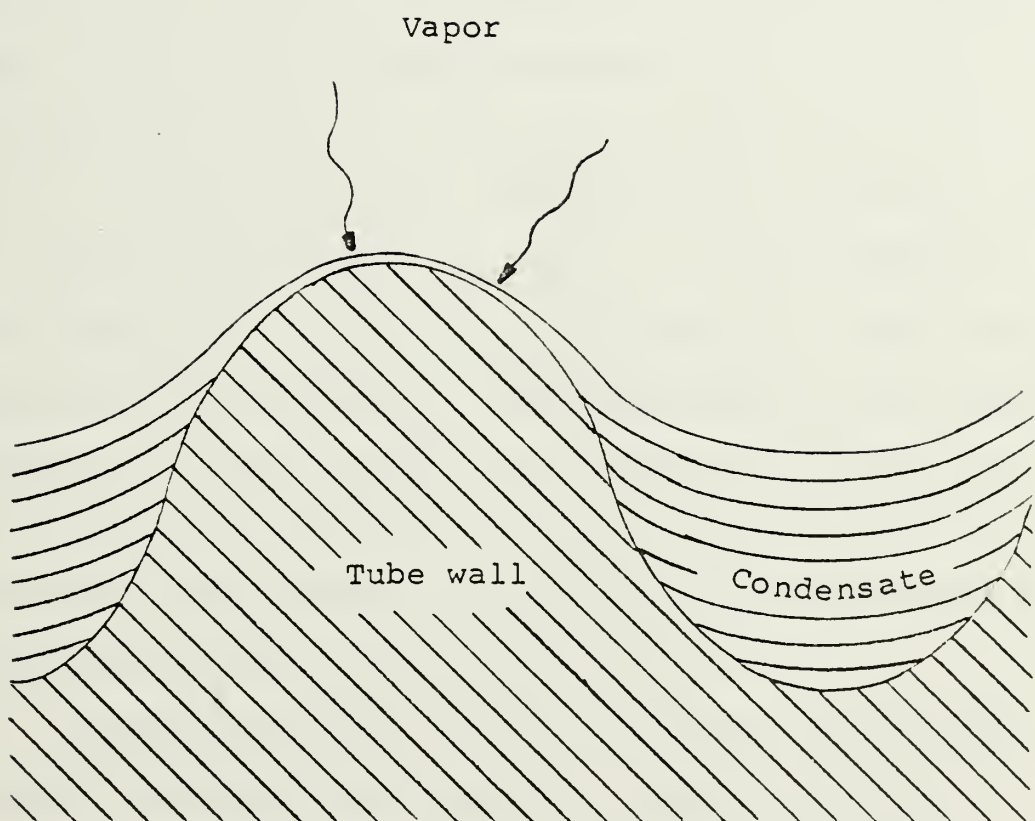


Figure I-2: Fluted surface concept

are avoided which could be sources of unexpected failure when the vessel is subjected to extremes of pressure, mechanical shock, or thermal shock.

The fluted surface having a sine geometry was analyzed by Yamamoto and Ishibachi using the Gregorig model [12]. Their analysis enables the calculation of an average condensate film thickness on the surface of the flute. The problem then reduces to one of balancing heat transfer and condensate mass flow. The phenomenon of the condensate filling the valley region of the flute is referred to as "flooding," and this concern for flooding presents the same problems as inundation of horizontal or vertical smooth tubes. Panchal and Bell considered the downstream effects of condensation as the valley of the flute begins to fill [13].

Proposing an alternative condenser design which simply re-orient the tubes and enhances their outer surfaces should accomplish the goals of being smaller and lighter. Condenser design considering alternative materials must be treated as part of the problem. Materials which warrant consideration are Copper-Nickel (Cu-Ni) 90-10, Cu-Ni 70-30, and Titanium, commercially pure, grade 2 (Ti, CP, Gr2). There are trade-offs for the use of these materials, the most important of which are strength and weight versus thermal conductivity.

In summary, the objective of this thesis is to present a methodology for a marine condenser design which has vertical fluted tubes and is possibly fabricated from different materials. This condenser must be lighter and smaller than existing condensers to warrant its manufacture and installation.

C. Design Inputs

Constraints for a condenser design can vary widely. For a marine condenser, these degrees of freedom are somewhat narrower, and the design process is governed by the concerns for weight, volume, and thermal efficiency. For naval condensers, reference [11] further limits the degrees of freedom in design. These limitations arise because of the requirements for the naval vessel to be able to operate effectively in varying environments.

The heat transfer requirements are for the conservation of energy from the condensation side of the condenser, through the tube wall, and into the cooling water. Thus the heat transfer characteristics can be analyzed separately for these three different regions.

1. Cooling water.

Various correlations, such as McAdams, Colburn, or Seider-Tate can be used to determine the heat transfer coefficient for turbulently flowing cooling water [6]. Fundamental non-dimensional groups which determine the cooling fluid heat transfer coefficient are the Reynolds number and the Prandtl number. The design parameters which govern these numbers are temperature dependent fluid properties, velocity, mass flow, and tube hydraulic diameter.

2. Tube Wall.

Heat transfer resistance through the tube wall is dependent upon tube material, wall thickness, and a scaling allowance.

3. Condensing Fluid.

The heat transfer coefficient on the condensing side of the tube will be shown to be a function of three non-dimensional groups. These groups are specified by surface geometry, condensing pressure (or temperature), and condensate drainage requirements [7, 12, 13].

Structural limitations are also defined in reference [11]. These are the source of considerable conflict with the heat transfer requirements. The desireable high

strength materials generally possess lower thermal conductivities and/or inferior metallurgical performance in salt water than lower strength pure alloys. Table I-1 gives a brief comparison for several common copper, nickel, and titanium based alloys. Stiffeners are also necessary to prevent excessive tube vibrations. These stiffeners may be used to provide condensate drainage strippers, but their spacing affects the condensation heat transfer coefficient [13, 14].

Power available for cooling water is a constraint which also affects the condenser design. Given a specific pump/motor limitation, by either size or power available, the velocity and mass flow of coolant are constrained. Heat losses through the condenser are determined by physical shape of the condenser, i.e., number of passes, baffles, etc., tube length, and the Reynolds number. As the tube length of the condenser decreases, a commensurate amount of pumping power becomes available for either increased coolant mass flow, or increased coolant velocity [15].

An itemized listing of design parameters for a marine condenser can be specified as follows [16]:

Table I-1
Thermal Conductivity and Yield Strength of
Several Common Metals and Select Alloys
[17,18]

<u>Metal/Alloy*</u>	<u>Thermal Conductivity</u>	<u>Yield Stress**</u>
	[BTU/hr ft °F]	[ksi]
Cu	230	~ 4.8
Cu-Ni 90-10	23	16
Cu-Ni 80-20	21	16
Cu-Ni 70-30	17	25
Ni (98.9% Pure)***	47	16
Monel 400 (66.5 Ni-31.5 Cu)	14	45-25
Monel 500 (66.5 Ni-29.5 Cu- 2.7Al-0.6Ti)	10	111
Ti (Cp-Gr 2)	11.4-9.5	40
Ti-5Al-2.5Sn	4.5-4.3	120
Ti-6Al-4V	3.8	120

*Properties are for 50°F < T < 100°F, annealed condition.

**Yield stress is defined for .2% deformation.

***Nickel and Ni-Cu alloys are unsuitable for marine tubing
because they are subject to deep pitting in seawater at
low velocities [23].

1. Tube material and material properties.
2. Tube geometry.
 - a. Inside diameter, outside diameter, and wall thickness;
 - b. Flute pitch and amplitude and nominal diameter.
3. Coolant characteristics.
 - a. Inlet temperatures;
 - b. Mass flow;
 - c. Velocity;
 - d. Physical and thermal properties.
4. Condenser operating conditions.
 - a. Condenser pressure;
 - b. Condensate temperature and mass flow;
 - c. Heat transfer requirements.
5. External requirements.
 - a. Tube length;
 - b. Tube bundle lay-out;
 - c. Number of passes;
 - d. Operating depth and safety factors;
 - e. Tube sheet and stiffner connections;
 - f. Air ejector locations;
 - g. Pumping power available or allowable head loss.

CHAPTER II

TUBE SELECTION

A. Materials

The materials which will be considered for marine condenser tubing are the copper-nickel alloys, Cu-Ni 90-10 and Cu-Ni 70-30, and commercially pure titanium, grade 2 (Ti, Cp). These materials are of interest because the U.S. Navy uses both Cu-Ni alloys [11], and Ti is a possible alternative material which will provide considerable weight savings. Table II-1 lists the mechanical and thermal properties of these materials along with their compositions [17,18].

In selecting a material for use in a condenser, several environmental factors must be considered. These include corrosion characteristics and wear properties of the material in a salt water environment, effects of biological fouling, and galvanic coupling.

1. Cooling water velocity effects.

The effects of sea water velocity on various metals is summarized in Figure II-1.

a. Copper-Nickel Alloys.

Cooling water velocity is one of the more important factors that affect Cu-Ni condenser tube deterioration.

Table II-1

Mechanical Properties and Composition of
Marine Condenser Materials [17,18]

<u>Alloy/Metal</u>	<u>Designation</u>					
	<u>Composition</u>					
	<u>Cu</u>	<u>Ni</u>	<u>Pb</u>	<u>Fe</u>	<u>Zn</u>	<u>Mn</u>
Cu-Ni 90-10	rem	9-11	0.05max	1-1.8	1.0max	0.5max (total)
Cu-Ni 70-30	rem	29-33	0.05max	0.4-0.7	1.0max	0.5max (total)
Ti CP						
	<u>Ti</u>	<u>N</u>	<u>C</u>	<u>H</u>	<u>Fe</u>	<u>Others</u>
Cu-Ni 90-30	rem	0.03max	0.10max	0.015max	0.30max	0.25max
Ti CP						
	<u>Properties</u>					
	$\frac{E}{(10^{+3} \text{ ksi}) (10^{+3} \text{ ksi})}$	$\frac{G}{(10^{+3} \text{ ksi}) (10^{+3} \text{ ksi})}$	$\frac{Y_S}{(\text{ksi}) (1 \text{ lbm/in}^3)}$	$\frac{P}{(\text{BTU/1lbm}^\circ\text{F}) (10^{-6} /^\circ\text{F})}$	$\frac{C_p}{(\text{BTU/hr ft}^\circ\text{F}) (10^{-6} /^\circ\text{F})}$	$\frac{K}{\alpha}$
Cu-Ni 90-10	20	7.5	16	.323	.09	23
Cu-Ni 79-30	22	8.3	25	.323	.09	17
Ti CP	15	6.0	40	.163	.125	9.5-11.4
						4.8

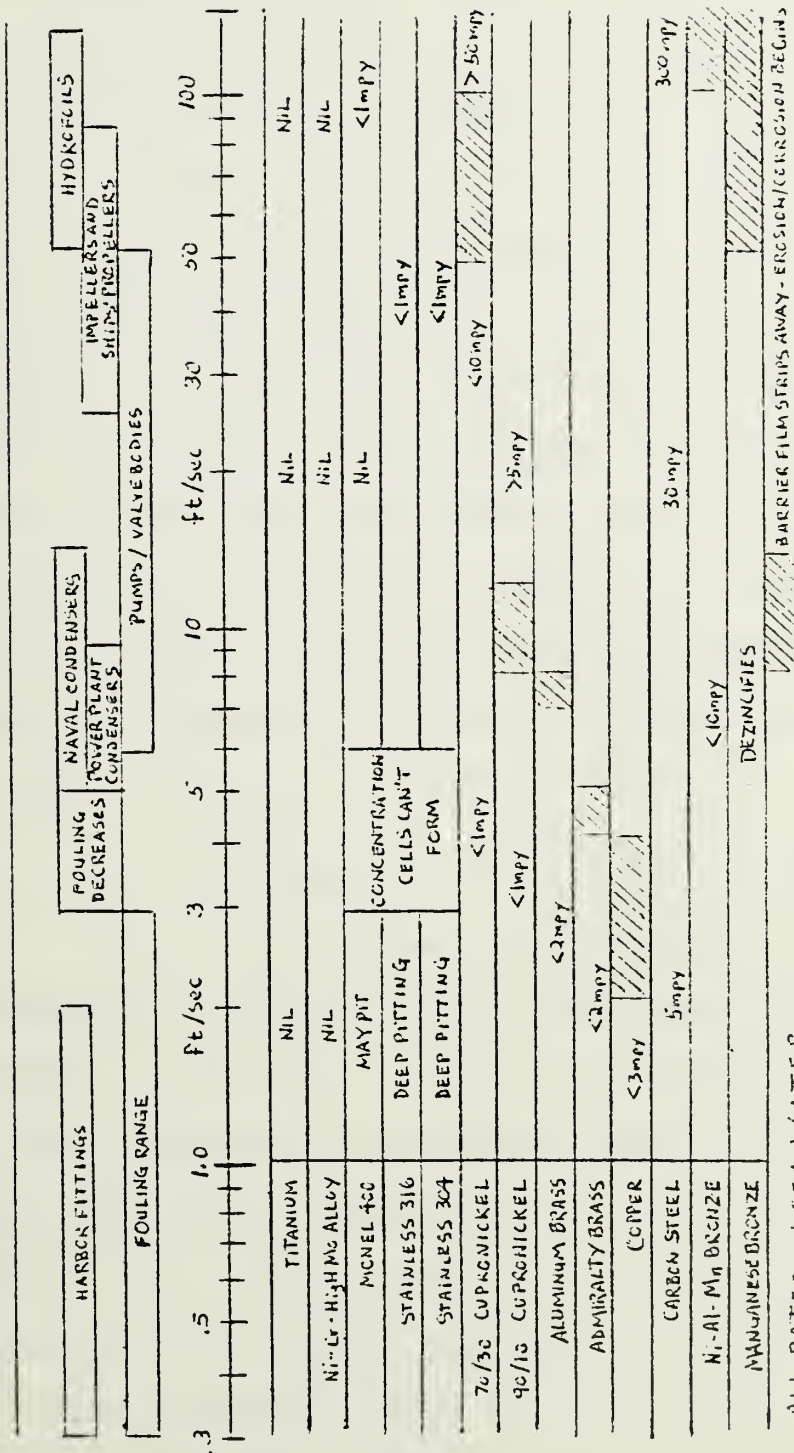


Figure II-1 - The Effects of Sea Water Velocity on Corrosion Resistance of Various Metals (23). (mpy = mils per year)

For these materials, a minimum velocity exists below which stagnation occurs and crevice corrosion is likely. Above a maximum critical velocity pitting and erosion occur. For Cu-Ni 70-30 this lower velocity limit is approximately 2-3 ft/sec, allowing for crevices on the order of 1.0 mil per year (mpy) [19,20,21]. Crevice corrosion characteristics for Cu-Ni 90-10 are similar to Cu-Ni 70-30 [22]. Various values are reported for maximum critical velocities, above which impingement attack and erosion occur. The maximum sea water velocity of 11 ft/sec, specified by reference [11] is less than the generally accepted critical velocity for the Cu-Ni alloys which is 12-15 ft/sec [20,22].

b. Titanium

Ti is very immune to the effects of velocity. This behavior is attributed to a chemically stable, rapidly formed, oxide film. Passivation occurs rapidly, even in the presence of mechanical damage such as a scratch. The oxide film "repairs itself" virtually instantaneously [21,22,23]. In sea water at velocities between 0-3 ft/sec, reported general corrosion rates are nil [21,23]. Crevice corrosion occurs with Ti only at temperatures above 250°F [23], and no corrosion occurs at sea water velocities up to 25 ft/sec and possibly greater [21].

2. Biological Fouling

In general, the more corrosion resistant metals and alloys are likely to experience biological fouling under slow moving conditions. Fouling by macro-organisms (mollusks, barnacles, etc.) has the obvious effect of reducing water flow, changing velocity profiles, and increasing pumping power requirements. Fouling by micro-organisms (algae, etc.) has the effect of adding another layer of thermal resistance to the inside of the tube wall [24].

a. Copper-Nickel Alloys

Water velocities in excess of about 5 ft/sec, temperatures above 120°F and below 50°F, low oxygen content or low food supply (such as in stagnant or closed systems) in the water will effectively prevent fouling of copper alloys by macro-organisms [20]. The copper alloys most resistant to all bio-fouling, however, are those containing more than 85 percent copper. Thus, even in a high velocity flow, some micro-biological fouling (referred to as "slime") will occur on Cu-Ni 70-30 surfaces due to bacterial and algae growth and adherance within the boundary layer [20,25,26,27]. The irritant or toxic effect of Cu²⁺ ions is believed to be the cause of reduced biological fouling on Cu-Ni alloy tubes [28].

b. Titanium

Since Ti is such an immune metal, biological fouling is a serious problem. The threshold velocity to prevent macro-biological fouling on Ti tubes is approximately 5 ft/sec [23,29]. Design of a system for active production of toxic agents must ensure that these agents are not environmentally hazardous. A chlorination system is acceptable to the environment, but the production of chlorine ions (Cl^-) is accompanied by hydrogen ions (H^+). Hydrogen ions are a hazard to titanium alloys, and except in the case of very pure metal can cause stress corrosion cracking [30].

3. Galvanic Coupling

When considering condenser materials, in the presence of a strong flowing electrolyte, namely sea water, galvanic effects are significant. The material itself, with its propensity to passivate, and the velocity of the sea water dictate the kinetics of corrosion due to galvanic coupling. Titanium is a much more active metal than copper, but it is because of this activity that it rapidly forms an oxide and becomes passive. Hence it is more noble than copper, and its general corrosion rates are much less. Table II-2 shows the relative nobility of various metals in flowing sea water, and it implies that Cu-Ni piping (used for

Table II-2

Galvanic Series of Metals in Flowing Sea Water [33]

Anodic or Least Noble

Magnesium and magnesium alloys
Zinc
Galvanized steel
Aluminum
Cadmium
Mild steel
Wrought iron
Cast iron
Stainless steel 304 (active), 316 (active)
Lead
Tin
Naval brass (60% copper, 39% zinc, 1% tin)
Copper
Red brass (85% copper, 15% zinc)
Copper-Nickel 90-10
Copper-Nickel 70-30
Nickel
INCONEL alloy 600 (78% nickel, 13.5% chromium,
6% iron)
Nickel aluminum bronze
Silver
Titanium
Stainless steel 304 (passive)
INCONEL alloy 625
HASTELLOY alloy C
MONEL alloy 400
Stainless steel 316 (passive)
INCOLOY alloy 825
Graphite
Platinum

Cathodic or Most Noble

most sea water piping) would deteriorate in the proximity and in contact with Ti [23,31]. Reference [11] requires zincs as cathodic protection in Cu-Ni tubed condensers since Cu is noble relative to steel. The steel is noble relative to the zincs, and they therefore corrode sacrificially. Such sacrificial anodes would definitely be required in a Ti tubed condenser [32]. In fact, the deterioration rate for such anodes might dictate an entire change in sea water piping systems to a more noble metal which would then exacerbate the biological fouling problem. Figure II-2 demonstrates this concern for cathodic protection requirements for a Ti tube condenser.

The significant variables for material use in condenser tubing, apart from strength requirements, are sea water velocity, galvanic effects, and susceptibility to biological fouling. The latter two of these are also functions of sea water velocity as shown in Figure II-1.

B. Strength Requirements

Reference [11] specifies for surface ship condensers a minimum tube wall thickness of .049 in. with Cu-Ni 90-10 alloy. The tube outside diameter is also specified as 5/8 (.625) in. Appendix A shows the

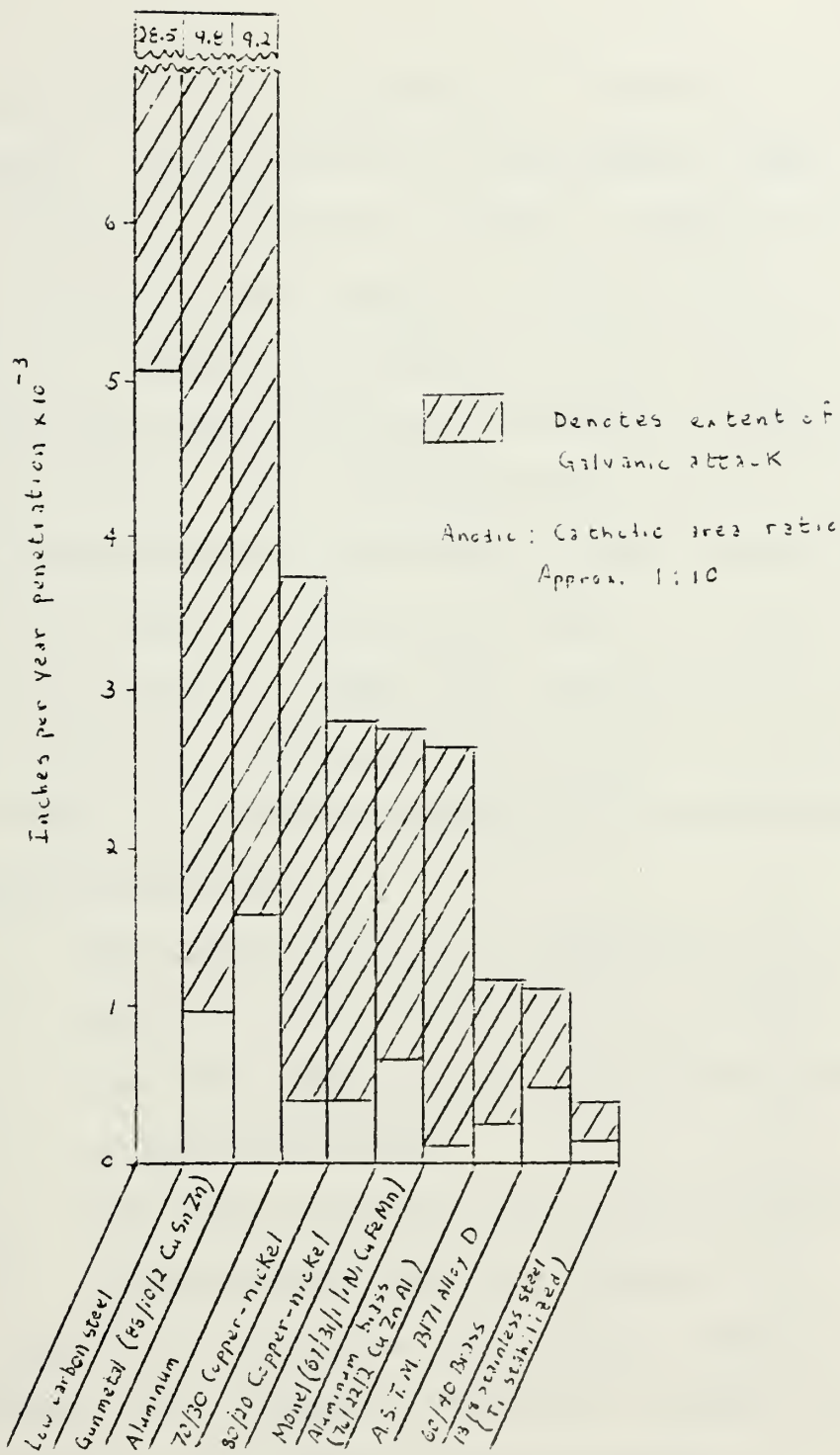


Figure II-2 - Behavior of Titanium metal couples immersed in aerated sea water for 2500 hrs. (32).

calculations required to determine condenser tube wall thickness. These results are presented as Table II-3. The minimum wall thickness allowed in practice for Cu-Ni 70-30 is 0.049 in. and for Ti is 0.035 in. [34]. Thus, from Table II-3. replacing Cu-Ni 90-10 with Cu-Ni 70-30 Ti is most practical strictly from a strength consideration for a surface ship. Other considerations, such as increased erosion protection in the face of a high velocity may force the change in materials as shown in Figure II-1.

The question of tube wall thickness for a submarine condenser is complicated by security requirements. These can be treated academically by the following conservative assumptions:

1. The design depth of a submarine is not the depth at which it operates. A safety factor has been applied which may be either additive or multiplicative.
2. The yield criterion for tube wall material also incorporates a factor of safety.

Appendix A shows the calculations required to produce Table II-3. Table II-3 presents various condenser tubes required for different design depths.

Table II-3
Tube Specifications for Various Design Depths*

<u>Design Depth (ft)</u>	<u>Material</u>	<u>OD (in)</u>	<u>t (in)</u>	<u>Gauge</u>
1050	Cu-Ni 90-10	.625	.049	18
1050	Cu-Ni 70-30	.625	.028	22
1050	Ti CP	.625	.019	--
1500	Cu-Ni 90-10	.625	.083	14
1500	Cu-Ni 70-30	.625	.049	18
1500	Ti CP	.625	.028	22
2000	Cu-Ni 90-10	.625	.109	12
2000	Cu-Ni 70-30	.625	.065	16
2000	Ti CP	.625	.035	20
2500	Cu-Ni 70-30	.625	.083	14
2500	Ti CP	.625	.047	18
3000	Cu-Ni 70-30	.625	.095	13 ⁺
3000	Ti CP	.625	.058	17
1050	Cu-Ni 90-10	.500	.035	20
1050	Cu-Ni 70-30	.500	.028	22
1050	Ti CP	.500	--	--
1500	Cu-Ni 90-10	.500	.065	16
1500	Cu-Ni 70-30	.500	.035	20
1500	Ti CP	.500	.022	--
2000	Cu-Ni 90-10	.500	.083	14
2000	Cu-Ni 70-30	.500	.049	18
2000	Ti CP	.500	.028	22
2500	Cu-Ni 70-30	.500	.065	16
2500	Ti CP	.500	.035	20
3000	Cu-Ni 70-30	.500	.083	14
3000	Ti CP	.500	.049	18

*Thickness for tubes has been rounded to the nearest even gauge except as noted by +.

CHAPTER III

ELEMENTS OF HEAT TRANSFER

Nomenclature

a	amplitude of the flute (ft)
A	area (ft^2)
B	dimensional group defined in eq. (III-7) ($ft/\text{°F}$)
C, C_p	specific heat (BTU/lbm °F)
D	diameter (ft)
F	number of flutes on the tube surface
g_c	gravitational constant (lbm ft/lbf hr 2)
G	mass flux (lbm/ ft^2 hr)
h	heat transfer coefficient (BTU/hr ft 2 °F)
h_{fg}	latent heat (BTU/lbm)
K	thermal conductivity (BTU/hr ft °F)
L	length (ft)
M	non-dimensional group defined in eq. (III-16)
Nu	Nusselt number
p	pitch of the flute (ft)
P	pressure (lbf/ ft^2) or (in-hg-abs)
Pr	Prandtl number
q	heat flow (BTU/hr)
r	radius of curvature of the fluted surface (ft)

R	thermal resistance (hr ft ² °F/BTU)
Re	Reynolds number
S _v	flute half perimeter (ft)
S _c	flute arc length on which condensing occurs (ft)
t	tube wall thickness (ft)
T	temperature (°F)
ΔT	T _S - T _W (°F)
U	overall heat transfer coefficient (BTU/hr ft ² °F)
V	velocity (ft/hr)
W	axial mass flow of liquid (lbm/hr)
s	tube surface coordinates
y	
z	

Greek letters

α	height of the condensate in the center of the flute (ft)
Γ	mass flow rate in S direction per unit length (lbm/hr ft)
δ	condensate film thickness (ft)
θ	angular representation of a point along the flute surface

μ	dynamic viscosity (lbm/hr ft)
ρ	density (lbm/ft ³)
σ	surface tension (lbf/ft)
Φ	non-dimensional group defined in eq. (B-12)
Ω	non-dimensional group defined in eq. (III-7)

Subscripts

b	at bulk temperature
c	coolant
D	referenced to hydraulic diameter
f	at flooding conditions
i	inside
n	nominal
o	outside
s	saturation
w	wall
sc	scale

Symbols

-	average
---	---------

A. Heat Transfer Coefficient of Cooling Water

No simple analytical solution exists for heat transfer in turbulent pipe flow. The McAdams correlation (or Dittus-Boelter equation) is widely accepted for the determination of the heat transfer coefficient for the cooling water [6,39].

$$\left(\frac{h_D}{K_b}\right) = 0.023 \left(\frac{G_D}{u_b}\right)^{0.8} \left(\frac{\mu C_p}{K}\right)_b^n \quad (\text{III-1})$$

or

$$Nu_D = 0.023 \left(Re_D\right)^{0.8} (Pr)_b^n \quad (\text{III-1a})$$

where

- 1) $n = 0.3$ if the fluid is being cooled
 $= 0.4$ if the fluid is being heated
- 2) all fluid properties are evaluated at the average (or bulk) fluid temperature
- 3) $2300 < Re_D < 10^7$ where
 Re_D \equiv Reynolds number based upon the hydraulic diameter
- 4) $0.5 < Pr_b < 120$ where
 Pr_b \equiv Prandtl number based on bulk temperature
- 5) $L/D > 50$

For flow through a condenser tube, these conditions are usually met and equation (III-1) is used as a basic relationship.

B. Heat Transfer Coefficient for a Tube Wall

For materials such as pure copper which have extremely high values for thermal conductivity, the thermal resistance of the condenser tube wall is almost negligible. From Table I-1, it is apparent that the strength requirements for marine condenser tubes mandate the use of materials with relatively low thermal conductivities.

The thermal resistance of the tube wall is the reciprocal of the heat transfer coefficient of the wall. For a smooth (non-enhanced) tube, this may be written as:

$$R_w = \frac{1}{h_w} = \frac{\ln(D_o/D_i)D_{ref}}{K} \quad (III-2)$$

For a fluted tube, however, the nominal diameter is used in place of the outside diameter [40]. The nominal diameter is defined as:

$$D_n = D_o + 2a \quad (III-3)$$

This is shown in Figure III-1. Use of the nominal diameter will be shown to be reasonable for two reasons:

1. The size of the flute is small with respect to wall thickness. (This is exaggerated in Figure III-1).
2. Heat transfer is blocked by condensate at the bottom of the flute valley as shown in Figure III-2. [9].

Furthermore, it is convenient to work with the nominal diameter vice the outside perimeter when dealing with the heat flux and condensing heat transfer coefficient.

Equation (III-2) can be written as:

$$h_w = \frac{1}{\frac{\ln(D_n/D_i)}{K} \frac{D_n}{2}} \quad (III-2a)$$

C. Heat Transfer Coefficient for Condensation

The coordinate system for this analysis is schematically depicted in Figure III-2. The arc length, S , is calculated by

$$S = \int_0^{\theta} \frac{p}{2\pi} \left\{ 1 + \left(\frac{2\pi a}{p} \right)^2 \sin^2 \phi \right\}^{1/2} d\phi \quad (III-3)$$

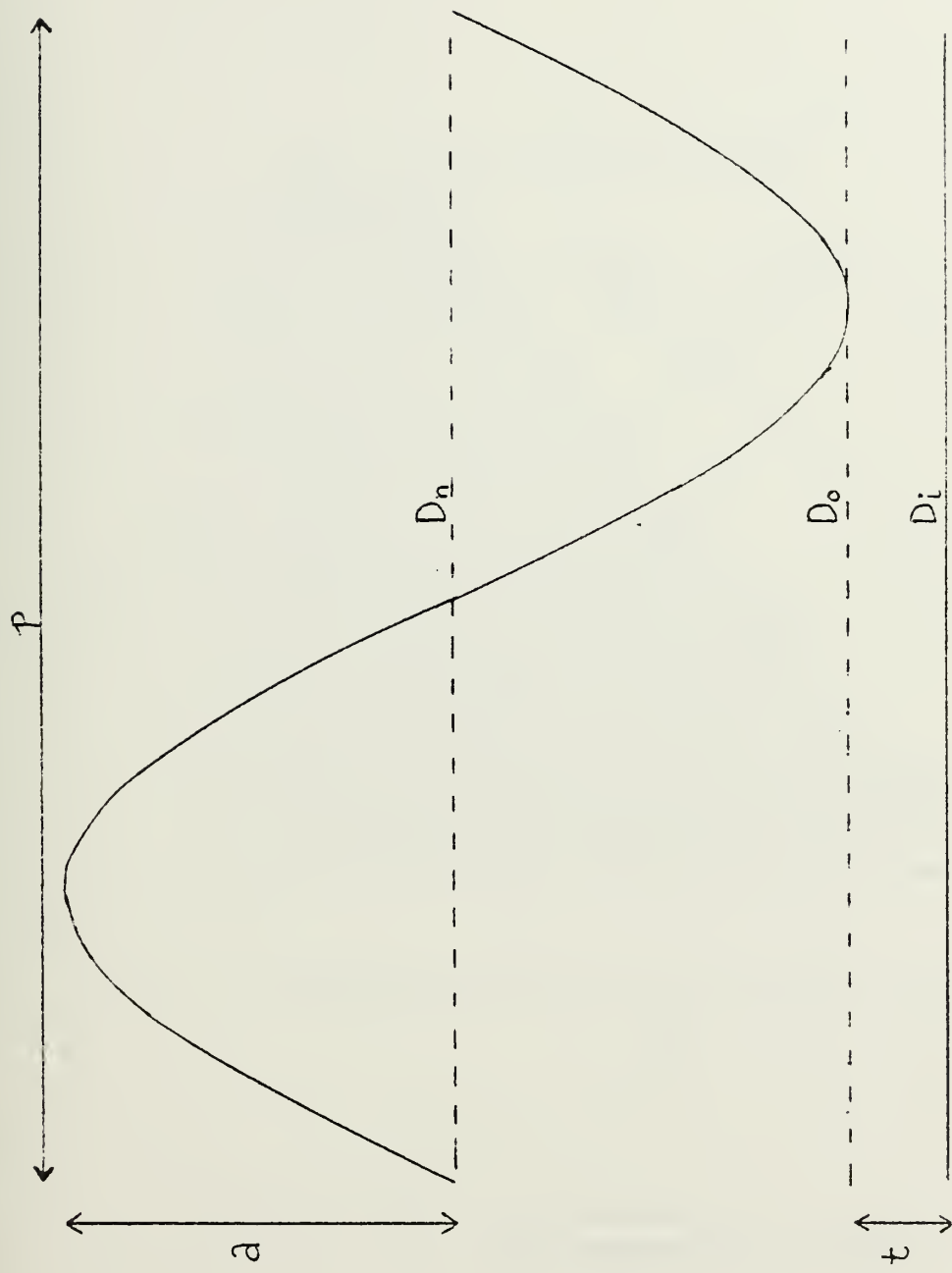


Figure III-1 - Schematic showing flattened tube dimensions

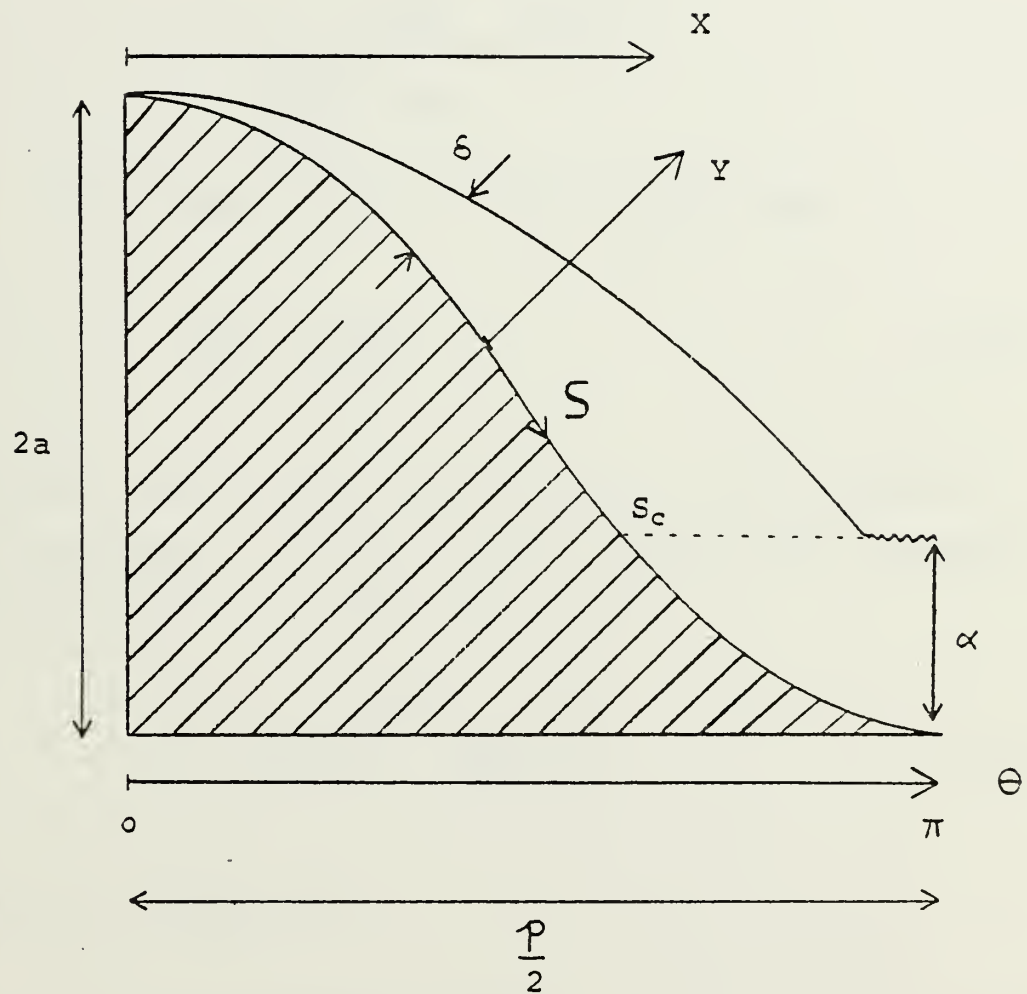


Figure III-2: Coordinates for flute and condensate profile

The radius of curvature of the fluted surface which has a sine geometry is

$$r = \frac{a \left\{ 1 + \left[\frac{2\pi a}{p} \right]^2 \sin^2 \theta \right\}^{3/2}}{\left(\frac{2\pi a}{p} \right)^2 \cos \theta} \quad (\text{III-4})$$

From Figure III-3 it can be shown that

$$\frac{dp}{ds} = \frac{d}{ds} \left(\frac{\sigma}{r} \right) \quad (\text{III-5})$$

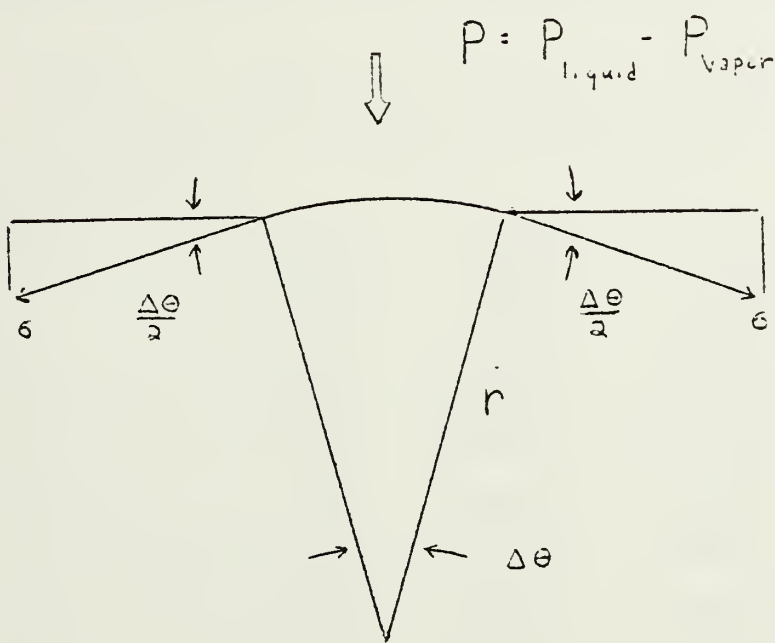
Appendix B shows that the equation for the condensate film thickness, δ , for a curved surface with a surface tension induced pressure differential is

$$\Omega = -\frac{\delta}{3a} \frac{d}{ds} \left[\delta^3 \frac{d}{ds} \left(\frac{1}{r} \right) \right] \quad (\text{III-6})$$

where Ω is defined as

$$\Omega \equiv \frac{\mu K \Delta T}{\rho g h_f g_c a} = \frac{B \Delta T}{a} \quad (\text{III-7})$$

The steps for solving equation (III-6) are shown by Gregorig [7] and Yamamoto and Ishibachi [12]. The solution is presented in Appendix B. Sample calculations are shown in Table III-1.



$$\sum F_r = 0 = Pr\Delta\theta - \sigma \sin\theta/2 \times 2$$

$$\sum F_\theta = 0 = \sigma \cos\theta/2 - \sigma \cos\theta/2$$

Figure III-3- Schematic of fluid surface showing force balance between pressure and surface tension.

Table III-1
Sample Calculations for Condensate Film Thickness

n	a/p	.15	.35	.45	.55
	$\delta_n \times 10^5$ ft				
0		1.5811	.4878	.3262	.2422
5		1.7219	.6673	.5436	.4802
10		2.0708	1.1451	1.0717	1.0522
15		2.5861	1.8466	1.8404	1.8785
20		3.1842	2.6712	2.7420	2.8451
25		3.7202	3.4183	3.5596	3.7215
30		4.0099	3.7606	3.9258	4.1083
35		3.9580	3.5078	3.6242	3.7693
40		3.6563	2.8574	2.8858	2.9616
45		3.2976	2.1107	2.0450	2.0468
50		3.0909	1.4664	1.3067	1.2374
55		3.4029	1.1087	.8361	.6900
60		6.7751	1.8444	1.2311	.8894

$$a = 2.00 \times 10^{-3} \text{ ft}$$

$$\Omega = 3.7649 \times 10^{-9}$$

$$\Delta\theta = \pi/60$$

$$\delta_n = f(n\Delta\theta)$$

From the results of equation (III-6), solved for the arc length $S_c = S_v$, Nu_o can be calculated as shown in Appendix B. A non-dimensional number, $Nu_o \Omega^{1/4}$, can be calculated, and from equation (III-6) and the definition of Nu_o ,

$$Nu_o \Omega^{1/4} = f(a/p) \quad (III-8)$$

This result is presented in Table III-2 and plotted in Figure III-4.

At a distance Z down the tube, condensate W runs down the flute, and the thickness of this condensate, α (Figure III-2), increases with Z . Here the heat transfer is neglected in the valley of liquid thickness α , and the integration of equation (III-6) stops at $S = S_c$. S_c is determined by equation (III-3) and θ_c .

$$\theta_c = \pi \left(1 - \frac{\alpha}{2a} \right) \quad (III-9)$$

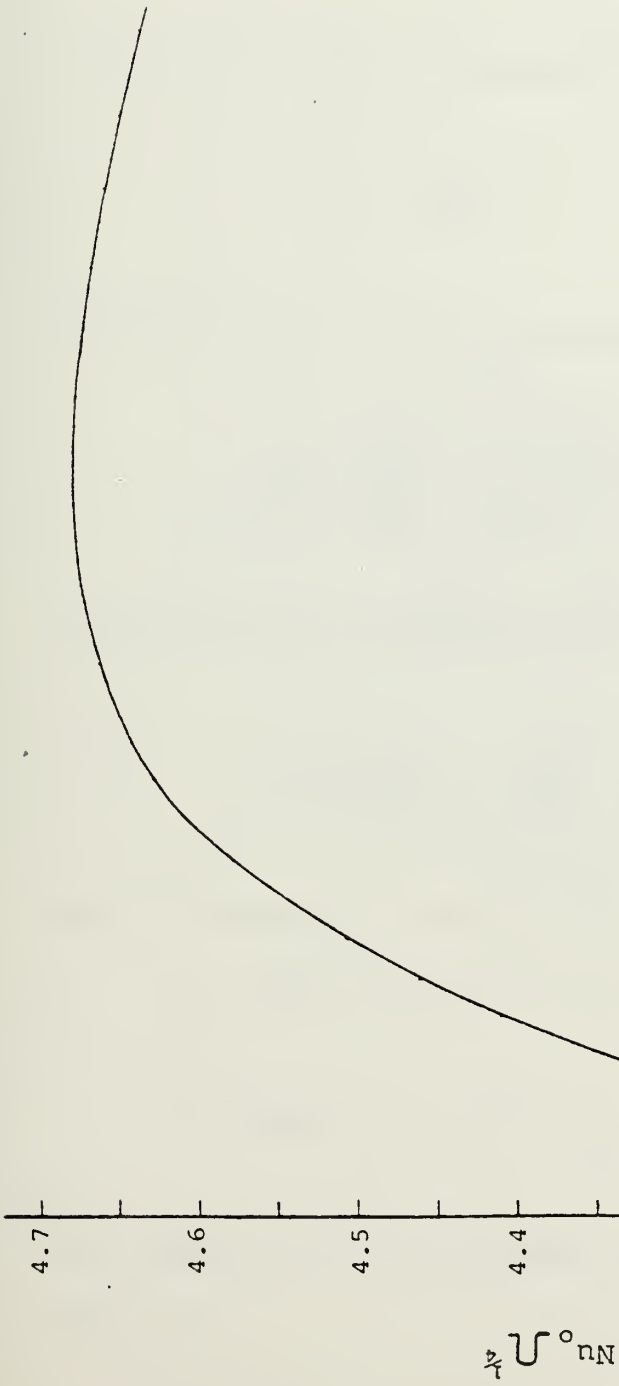
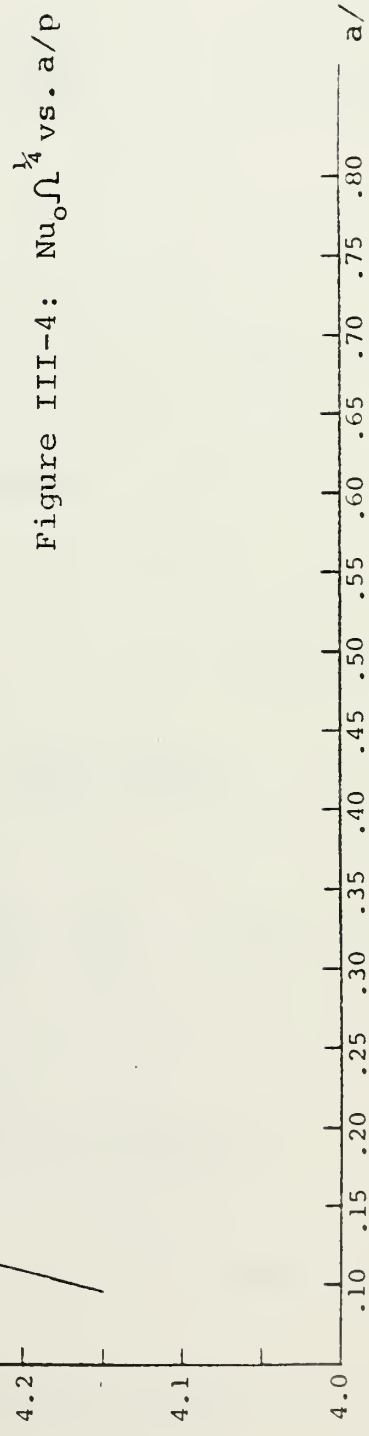
When $\alpha = 2a$ the valley is flooded [13], and $W = W_f$ where

$$W_f = 2g \frac{\rho^2}{\mu} (2a)^4 \left[36 \frac{a}{p} \exp \left\{ 3.33 \frac{a}{p} \right\} \right]^{-1} \quad (III-10)$$

Table III-2

Sample Calculations for $Nu_{\infty}^{1/4} = f(a/p)$

<u>$a \times 10^3$ (ft)</u>	<u>a/p</u>	<u>Nu_{∞}</u>	<u>$\alpha \times 10^9$</u>	<u>$Nu_{\infty}^{1/4}$</u>
10.0	.1	532.31	3.7649	4.1697
5.0	.1	532.31	3.7649	4.1697
1.0	.1	532.31	3.7649	4.1697
2.0	.15	553.65	3.7649	4.3368
10.0	.25	326.54	37.649	4.5486
10.0	.25	580.68	3.7649	4.5486
10.0	.25	1032.62	.37649	4.5486
2.0	.25	580.69	3.7649	4.5486
2.0	.40	595.41	3.7649	4.6639
2.0	.45	596.89	3.7649	4.6755
2.0	.50	597.45	3.7649	4.6799
2.0	.55	597.36	3.7649	4.6792
2.0	.60	596.80	3.7649	4.6749
2.0	.65	595.92	3.7649	4.6680
2.0	.70	594.81	3.7649	4.6593
2.0	.75	593.55	3.7649	4.6494



or

$$w_f = \frac{8}{9} g \frac{\rho^2}{\mu} (a)^3 p \exp \left[-3.33 \left(\frac{a}{p} \right) \right] \quad (\text{III.10a})$$

A Reynolds number is defined [13] as

$$Re = \frac{4 w}{S_v \mu} \quad (\text{III.11})$$

Calculations by Panchal and Bell [13] show

$$\frac{w_z}{w_f} = \frac{Re_z}{Re_f} = \left(\frac{a}{2a} \right)^{3.252} \quad (\text{III.12})$$

From Appendix B and equations (III-9) and (III-12)

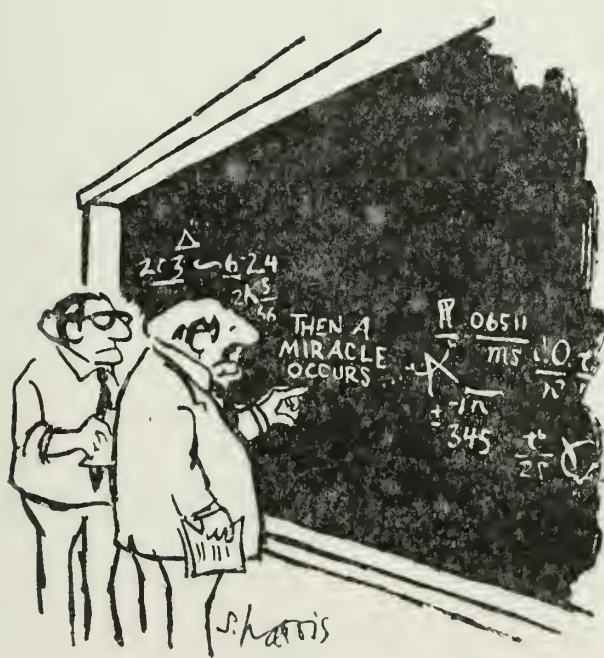
$$\frac{h_z}{h_o} = \frac{Nu_z}{Nu_o} = f \left(\frac{Re_z}{Re_f}, \frac{a}{p} \right) = f \left(\frac{w_z}{w_f}, \frac{a}{p} \right) \quad (\text{III.13})$$

This is shown by example in Figure III-5.

An energy balance on the tube surface requires

$$h_z dz \pi D_n \Delta T = h_{fg} dw \frac{\pi D_n}{p} \quad (\text{III.14})$$

This equation is re-arranged and integrated between $Z = 0$ and $Z = L$.



"I THINK YOU SHOULD BE
MORE EXPLICIT HERE IN STEP TWO."

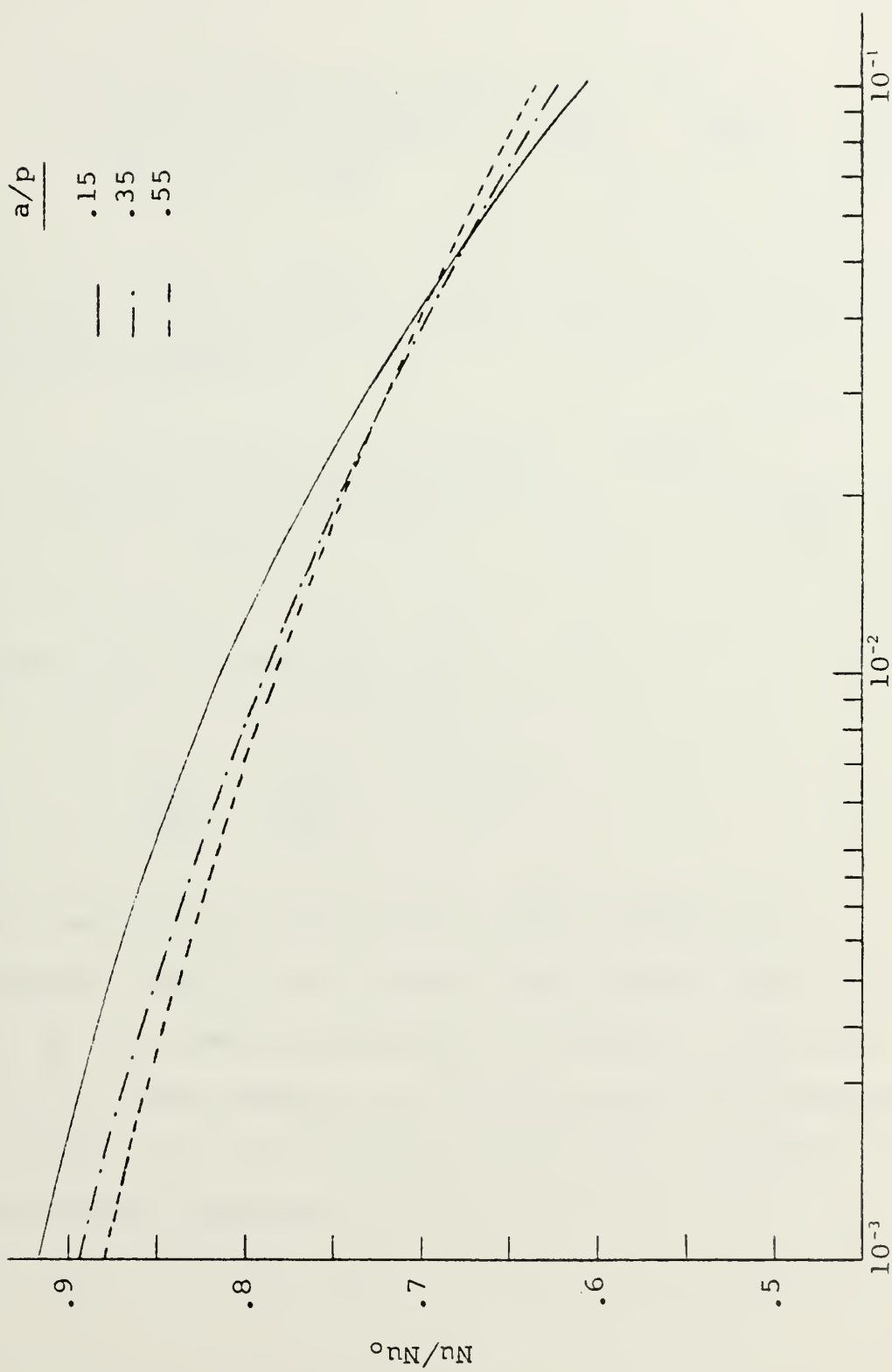


Figure III-5: Nu/Nu_0 vs. W/W_F

$$\frac{L p \Delta T}{h_{fg} W_f \text{Nu}_Z} \left(\frac{h_Z p}{K} \right) \frac{K}{p} \left(\text{Nu}_O \Omega^{1/4} \right) = \frac{\text{Nu}_O}{W_f} \int_0^{W_L} \frac{dW}{\text{Nu}_Z} \quad (\text{III.15})$$

By grouping the constants in the right-hand expression, M can be defined as

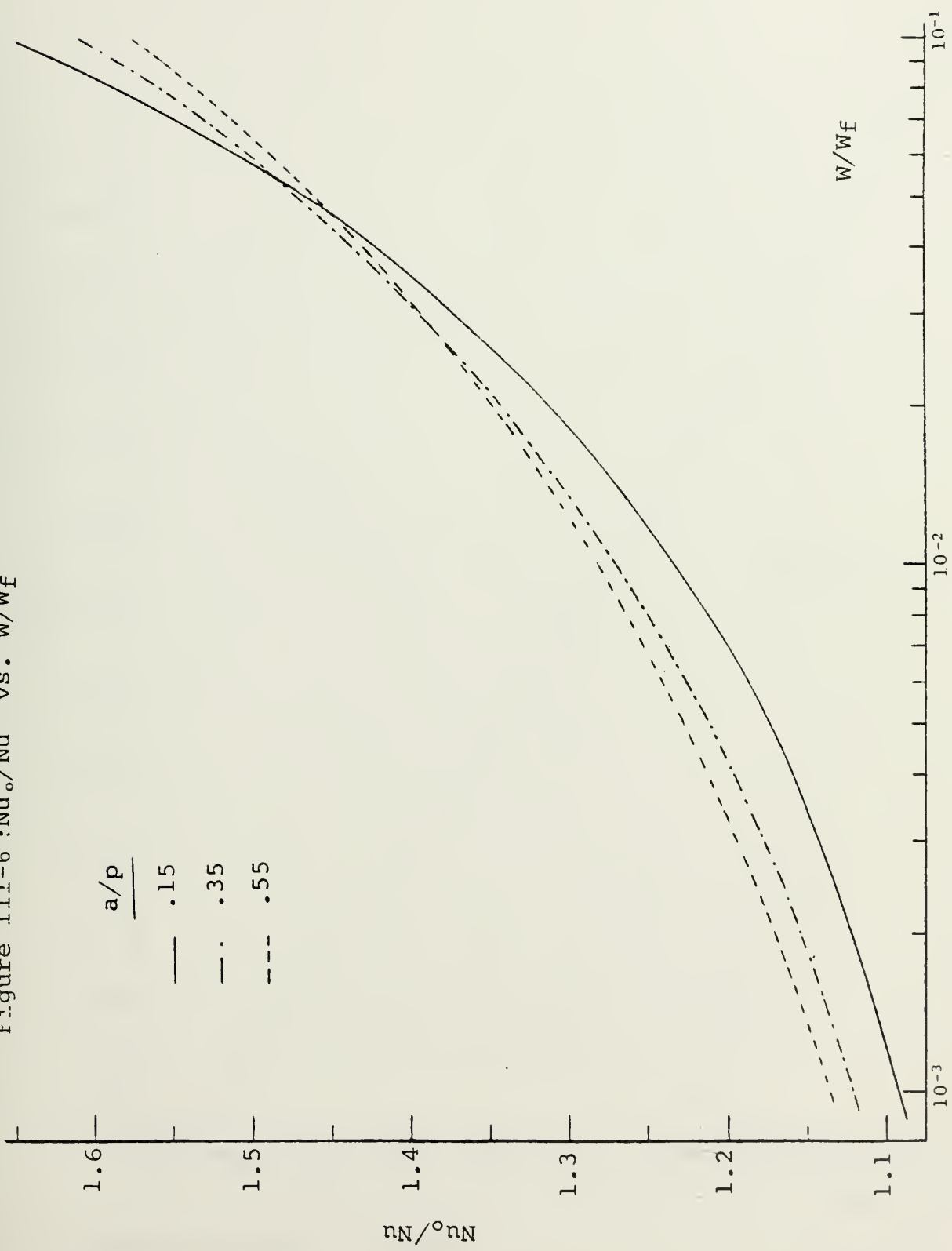
$$M \equiv \frac{K(a)^{1/4} \left(\text{Nu}_O \Omega^{1/4} \right) \left(L \Delta T^{3/4} \right)}{h_{fg} (B)^{1/4} W_f} = \int_0^{(W/W_f) L} \frac{\text{Nu}_O}{\text{Nu}_Z} d \left(\frac{W}{W_f} \right) \quad (\text{III.16})$$

Figure III-5 is replotted as

$$\frac{\text{Nu}_O}{\text{Nu}_Z} = f \left(\frac{W_Z}{W_f} \right) \quad (\text{III.17})$$

and presented as Figure III.6. The integral in equation (III.16) is evaluated from Figure III-6, and two of the cases are presented in Figures III-7a and III-7b. These results are also tabulated and presented as Table III-3. Note that the integration smooths out most of the dependency on (a/p) so that

Figure III-6 : Nu_o/Nu vs. W/W_f



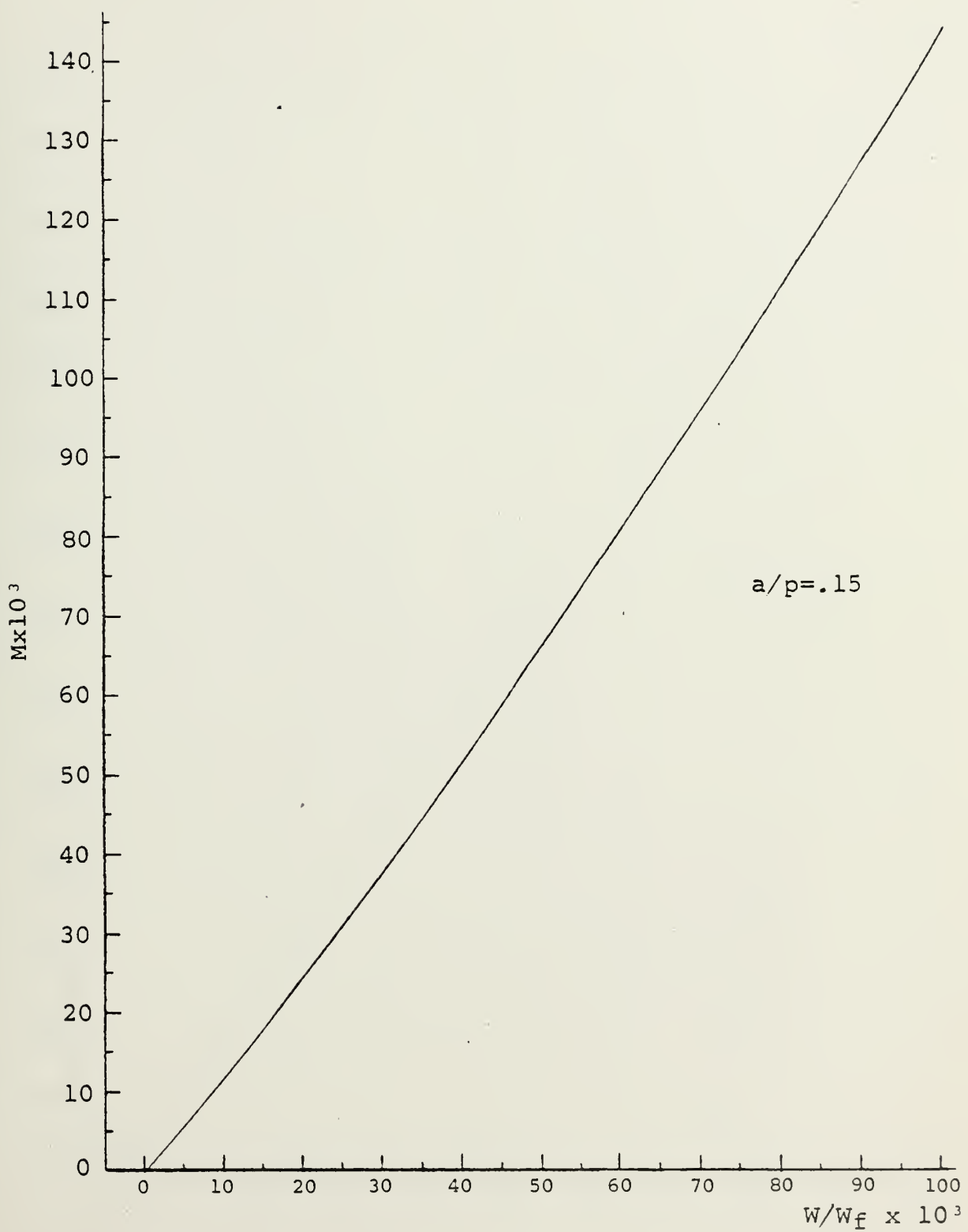


Figure III-7a: M vs. W/W_f

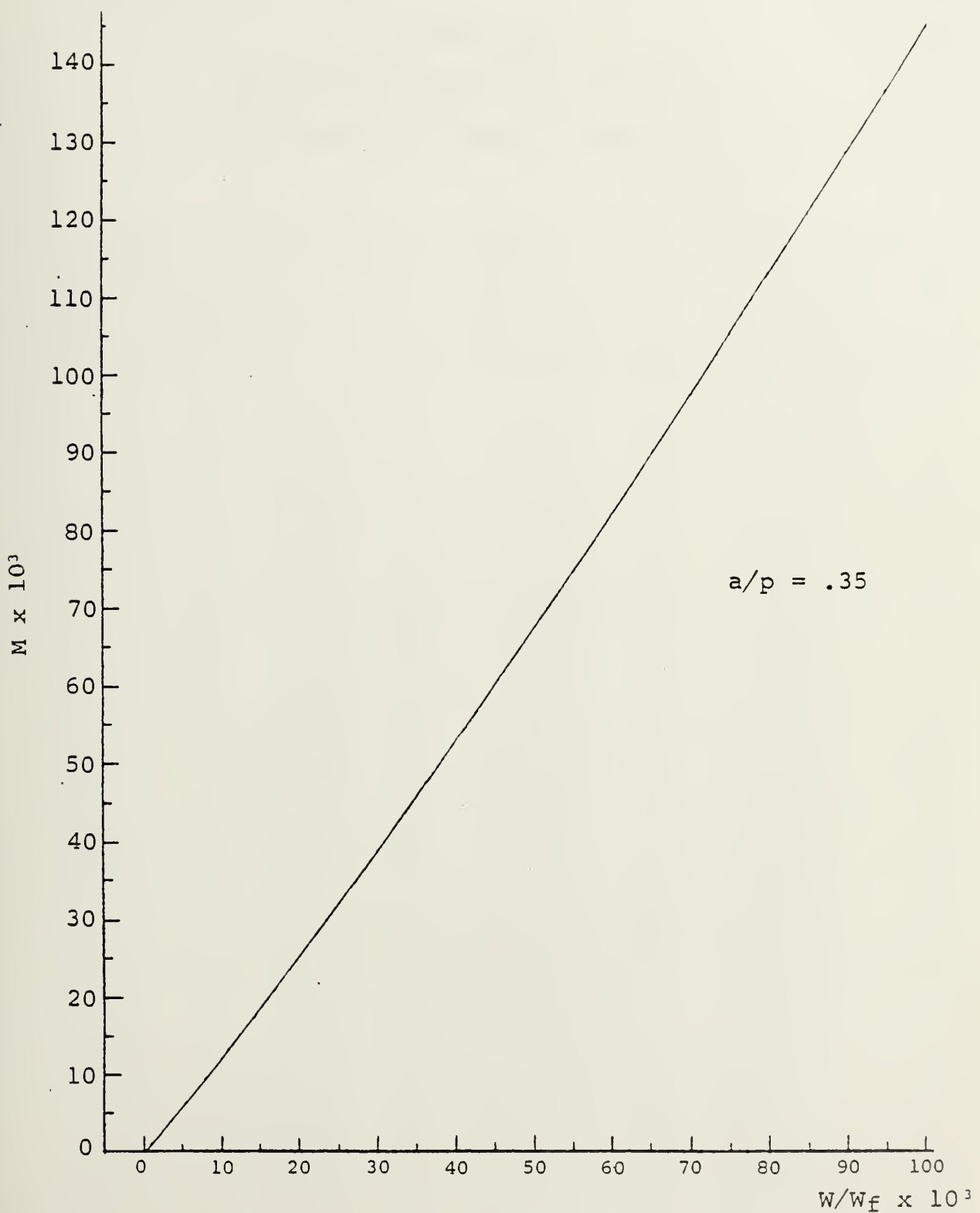


Figure III-7b: M vs. W/W_f

Table III-3
 Calculated Values for M and $\frac{W}{W_f}$
 for Several Different Values of a/p

$M \times 10^3$

$\frac{W}{W_f} \times 10^3$	a/p = .15	a/p = .35	a/p = .55
0	0	0	0
1	1.06	1.07	1.07
2	2.18	2.21	2.24
3	3.35	3.38	3.42
4	4.44	4.56	4.62
5	5.61	5.77	5.85
6	6.79	6.97	7.08
7	7.98	8.22	8.32
8	9.19	9.46	9.58
9	10.40	10.72	10.85
10	11.63	11.98	12.12
15	17.87	18.43	18.62
20	24.36	25.04	25.26
30	37.61	37.75	38.97
40	51.48	52.56	52.76
50	65.97	67.14	67.20
60	80.75	81.95	81.88
70	96.07	97.15	96.90
80	111.63	112.55	112.08
90	127.67	128.30	127.55
100	143.96	144.21	143.16
110	160.70	160.46	159.05

$$M = f (W/W_f) \quad (III.18)$$

$$M \neq f (W/W_f, a/p) \quad (III.18a)$$

The data in Table III-3 suggests a relationship for M such that

$$M = 1.7312 (W/W_f)^{1.0839} \quad (III.19)$$

for $W/W_f \geq 0.003$

The average heat transfer coefficient, \bar{h} , is defined as

$$\bar{h} \equiv \frac{(q/A_n)}{\Delta T} \quad (III.20)$$

which may be written as

$$\bar{h} = \frac{h_{fg} W_f}{p L \Delta T} \left(\frac{W}{W_f} \right) = \frac{h_{fg} W_f \cdot 6027 (M)^{.9226}}{p L \Delta T} \quad (III.21)$$

Substituting for M from equation (III.16) gives

$$\bar{h} = .6027 \left[\frac{h_f g w_f}{L \Delta T} \right]^{0.0774} a^{0.2307} \frac{[f(a/p)]^{0.9226}}{p} \left[\frac{K^3 \rho c h_f g g_c}{\mu \Delta T} \right]^{0.2307} \quad (\text{III.22})$$

where $f(a/p) = \text{Nu}_o \Omega^{1/4}$ from Figure III-4. At $L = 0$ this should show that $\bar{h} = \bar{h}_o$. The relationship for w/w_f and M fails for $w/w_f < 0.003$, and this equation for \bar{h} goes to ∞ .

D. Application to Condenser Design

In the design of a fluted condenser, it may be desirable to place stripper plates along the length to remove the condensate well before it reaches the flooding flow rate - perhaps keeping $w/w_f \leq 0.1$. Figure III-8 shows such stripper plates.

To determine L and w/w_f , a system of 4 equations must be solved. Other unknowns to this system of equations are: (q/A_n) , T_{c2} and ΔT . Therefore, one of these five variables must be specified. In practice, either L or w/w_f would generally be chosen. The system of equations is:

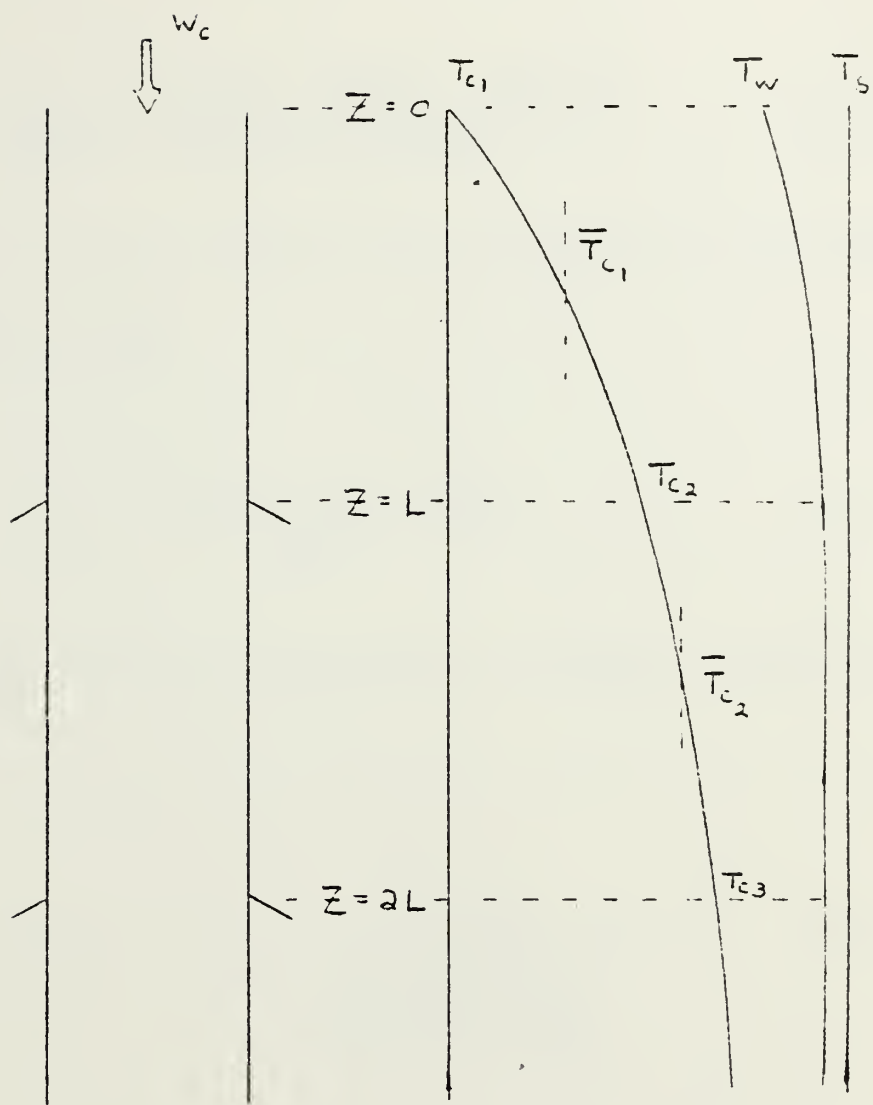


Figure III-8- Schematic diagram showing stripper plate spacing and axial temperature distribution.

$$1) \quad \left(\frac{q}{A_n}\right) = \frac{h_{fg} w_f (w/w_f) (\Delta T)^{3/4}}{p [L (\Delta T)^{3/4}]} \quad (\text{III.23})$$

which comes from the conservation of energy on one flute of the tube surface.

$$2) \quad \left(\frac{q}{A_n}\right) = \frac{w_c c_c (T_{c2} - T_{c1})}{\pi D_n L} \quad (\text{III.24})$$

which comes from the conservation of energy in the cooling water.

$$3) \quad \left(\frac{q}{A_n}\right) = U_{n,w} \frac{\frac{(T_{c2} - T_{c1})}{(T_s - \Delta T - T_{c1})}}{\ln \left[\frac{(T_s - \Delta T - T_{c1})}{(T_s - \Delta T - T_{c2})} \right]} \quad (\text{III.25})$$

which is the conservation of energy through the tube wall using an overall heat transfer coefficient and log mean temperature difference for the coolant.

$$\frac{1}{U_{n,w}} = \frac{D_n}{D_i} \left[\frac{1}{h_c} + \frac{1}{h_{sc}} \right] + \frac{\ln (D_n/D_i)}{K} \frac{D_n}{2} \quad (\text{III.26})$$

For short lengths or small temperature rises in the coolant, the log mean temperature difference may be replaced by

$$\frac{(T_{c2} - T_{c1})}{\ln \left[\frac{(T_s - \Delta T - T_{c1})}{(T_s - \Delta T - T_{c2})} \right]} \approx T_s - \Delta T - \bar{T}_c \quad (\text{III.27})$$

$$\text{where } \bar{T}_c = \frac{1}{2} (T_{c1} + T_{c2}) \quad (\text{III.28})$$

The fourth equation of the system comes from the definition of M in equation (III.16)

$$4) \quad \left[L(\Delta T)^{3/4} \right] = \frac{M w_f (B)^{1/4} h_{fg}}{(\text{Nu}_o^{\Omega})^{1/4} (a)^{1/4} K} \quad (\text{III.29})$$

where M is approximated by equation (III.19).

With L specified and w/w_f allowed to float, the solution to these equations is as follows:

- 1) Assume T_{c2}
- 2) Assume ΔT
- 3) Solve for (q/A_n) in equation (III.25)
- 4) Solve for (w/w_f) in equation (III.23)
- 5) Solve for M in equation (III.19)

6) Solve for ΔT in equation (III.29)

7) Repeat steps 3-6 until

$$|\Delta T_i - \Delta T_{i+1}| \leq \epsilon_{\Delta T}$$

8) Solve for T_{c_2} in equation (III.24)

9) Repeat steps 2-8 until

$$|T_{c_2j} - T_{c_2j+1}| \leq \epsilon_{T_{c_2}}$$

With w/w_f specified and L allowed to float, the solution to these equations is as follows:

1) Assume T_{c_2}

2) Assume L

3) Solve for ΔT in equation (III.29)

4) Solve for (q/A_n) in equation (III.25)

5) Solve for L in equation (III.23)

6) Repeat steps 3-5 until

$$|L_i - L_{i+1}| \leq \epsilon_L$$

7) Solve for T_{c_2} in equation (III.24)

8) Repeat steps 2-7 until

$$|T_{c_2j} - T_{c_2j+1}| \leq \epsilon_{T_{c_2}}$$

Table III-4 shows the results of these calculations for a typical condenser, neglecting thermal resistance in the wall. Appendix C shows the calculations for the solution to this system of equations as applied to a condenser design.

Table III-4
Sample Results for a Fluted Condenser*

Given: $D_o = .625$ in
 $t = .049$ in
 $Tc_1 = 75.0^\circ F$
 $v_c = 7.5$ ft/sec
 $w_c = 12000$ GPM (6.1513×10^6 lbm/hr)
 $a = 1.50 \times 10^{-3}$ ft
 $a/p = .31205$
 $P_c = 2.5$ in-Hg-abs
 $Nu_o \Omega^{1/4} = 4.612$
 $B = 4.3777 \times 10^{-12}$ ft/ $^\circ F$
 $D_n = 5.5083 \times 10^{-2}$ ft
 $P = 4.8069 \times 10^{-3}$ ft
 $F = 36$
No. of tubes = 2354
 $w_f = 5.4020$ lbm/hr

<u>Section</u>	1	2	3	4
ΔT ($^\circ F$)	1.084	0.764	0.523	0.350
w/w_f	0.10	0.079	0.060	0.046
L (ft)	3.252	3.252	3.252	3.252
$(q/A_n) (BTU/hr ft^2)$	35650	28000	21550	16300
Tc_2	83.17	89.59	94.53	98.26
$q_{total} = 1.345 \times 10^8$ BTU/hr				

*wall resistance neglected; cooling fluid is sea water.

E. Heat Transfer Resistance Due to Scaling

Allowance for dirt or scale can be made by either including separate thermal resistances for the scale or fouling associated with the tube material and fluid or by allowing a percentage reduction of the overall heat transfer coefficient, U . Reference [11] requires the latter method using a 15 percent reduction. Reference [6] recommends a straight allowance, regardless of material but dependent upon cooling medium. The value recommended for sea water is:

$$R_{sc} = \frac{1}{h_{sc}} = .0005 \text{ (hr ft}^2\text{F/BTU)}$$

Reference [41] recommends including a separate resistance for metal oxide on each side of the tube and a separate fouling resistance. This gives a value for U of the form,

$$\frac{1}{U_n} = \frac{1}{h_{\text{condensing}}} + \frac{D_n}{D_i} \frac{1}{h_{\text{sea water}}} + R_W + R_{\text{ox}} + R_f \quad (\text{III-31})$$

Values for R_{oxide} are listed in Table III-5. Since R_{fouling} is a virtual unknown and the quantity $2R_{\text{ox}} + R_f$ can be approximated for all cases in sea water as

$$2R_{ox} + R_f = R_{sc} \sim .0005 \text{ (hr ft}^2\text{°F) / BTU)}$$

This gives a value for U_n of the form

$$\frac{1}{U_n} = \frac{1}{h_{\text{condensing}}} + \frac{D_n}{D_i} \left[\frac{1}{h_{\text{sea water}}} + \frac{1}{h_{\text{scale}}} \right] + \frac{\ln \left(\frac{D_n}{D_i} \right) D_n}{K_{\text{tube}}^2} \quad (\text{III.32})$$

where $h_{sc} = 2000 \text{ BTU/hr ft}^2\text{°F}$.

TABLE III-5
Values of R_{ox} , the Resistance of the
Oxide Film on the Inside and Outside
Surfaces of Clean Tubes [41]

<u>Tube Material</u>	$R_{oxide} \left(\frac{hr ft^2 \circ F}{BTU} \right)$
Admiralty Metal	0.000136
Aluminum Bronze	0.000153
Aluminum Brass	0.000167
Cu-Ni 90-10	0.000178
Cu-Ni 80-20	0.000193
Cu-Ni 70-30	0.000243
Titanium	0.000195

CHAPTER IV
DESIGN PROPOSALS

A. Condenser Geometry

A primary objective of this work is to provide a methodology for a condenser design which allows the naval architect to specify condenser length. The naval architect is constrained by weight and volume, but the dimension which is most critical in marine plant layout is the tube length. The transverse area of the tube bundle can grow with significantly less impact on the other engineering systems than axial growth. By specifying the tube length, the maximum tube deflections and vibration characteristics can be predetermined. This allows the placement of tube and shell stiffeners which may also act as condensate stripper plates as suggested in Figure III-8. For typical spacing requirements of 1-8 feet, flutes with amplitude of 12-24 mils ($1.0 - 2.0 \times 10^{-3}$ ft) are predicted by this work. Appendix C demonstrates how a length may be specified for a condenser design. A typical double-pass fluted condenser drawing is shown in Figure IV-1.

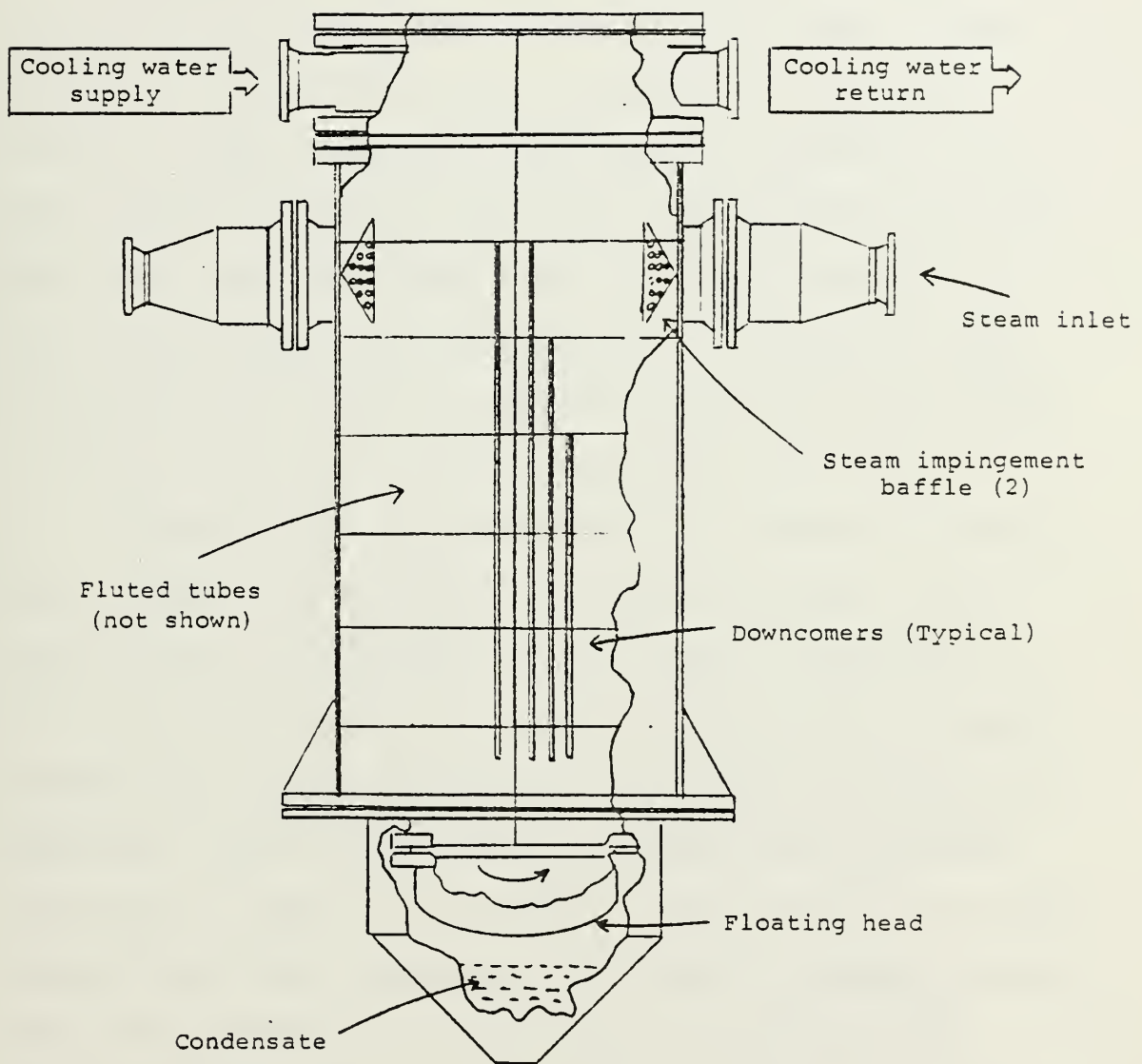


Figure IV-1: Possible configuration for a 2 Pass Vertical Condenser

B. Tube Attachment

A serious consideration for a naval condenser is the ability to pull and replace or plug tubes without having to remove the entire condenser or tube sheet. Tubes in naval condensers are usually attached to the tube sheets by rolling their ends and actually pressing them into the tube sheet [41,42]. This procedure is well established for Cu-Ni alloys, and rolled Ti tube-to-tube sheet joining procedures are being established to meet naval heat exchanger requirements [43].

Figure IV-2 is a drawing of a proposal to facilitate fluted tube attachment to the tube sheet while maintaining the ability to pull a tube if required.

As shown in Figure IV-2, a forged collar can be placed around the fluted surface at points where attachment is desired. This collar could be snugged into place by heating it, prior to attachment, and allowing it to cool around the tube. Reference [41] shows a similar attachment for ferrules to allow longitudinal expansion.

Reference [42] reports successful rolling of 5/8 inch diameter Ti tubes with 0.049 inch wall thickness. The composite wall thickness for a Ti tube with flute amplitude of 18 mils and tube wall thickness of 0.035 inches is 0.710 inches. This may pose a problem, and further research is warranted.

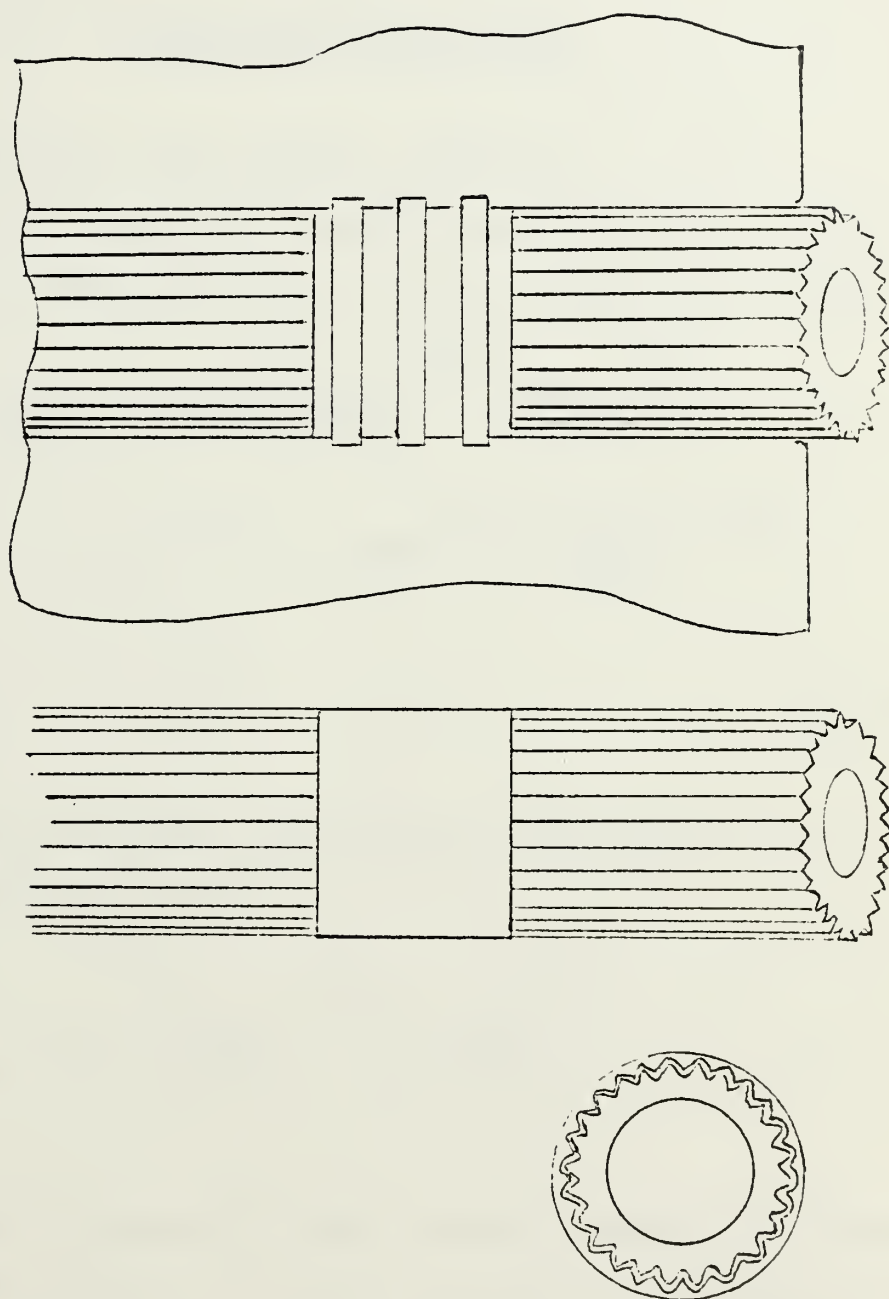


Figure IV-2 - A Proposed Method for Rolling Fluted Tubes into the Tube Sheet Showing a Shaped Band Around the Tube.

CHAPTER V

RESULTS AND CONCLUSIONS

A. Comparison with Nusselt analysis

The average heat transfer coefficient for condensation on a fluted surface is given by equation (III.22).

$$\bar{h}_{fl} = .6027 \left[\frac{K^3 \rho h_{fg}}{\mu \Delta T} \right]^{.2307} \frac{(\sigma g_c)^{.2307}}{p} \\ \times a^{.2037} [f(a/p)]^{.9226} \left[\frac{h_{fg} w_f}{L \Delta T} \right]^{.0774}$$

(III.22)

From the Nusselt analysis for condensation on a smooth vertical surface,

$$\bar{h}_{Nu} = .943 \left[\frac{K^3 \rho h_{fg}}{\mu \Delta T} \right]^{.25} \left[\frac{(\rho - \rho_v) g}{L} \right]^{.25} \quad (V.1)$$

These two equations show a much different dependence on the axial length L , but \bar{h}_{fl} is strongly influenced by pitch. ΔT also affects \bar{h}_{fl} more than \bar{h}_{Nu} . All other things being of a similar magnitude or extremely weak functions, \bar{h}_{fl} is dominated by p , ΔT , and a . The Nusselt analysis shows that \bar{h}_{Nu} is strongly affected by L and ΔT .

Figure V-1 is a graph relating the average heat transfer coefficient with length. Since M as defined in equation (III.16) is linear with L , the relationship between (w/w_f) , M , and L for a given \bar{h}_L (or $\bar{h}_L/h_o = \bar{N}u_L/Nu_o$) can be seen to be unique.

B. Condenser Comparison Using Titanium

To compare a Ti condenser with the Cu-Ni 70-30 condenser cited in Appendix C, another constraint must be included. Since the Ti tubes have thinner walls, less of them will be required for the sea water mass flow. This implies that the Ti condenser will either be longer or transfer less heat. An alternative is to allow the mass flow of the coolant to increase, i.e., increase the number of tubes. This will be the approach taken here so that the condenser length and overall heat transfer remain the same. Table V-1 shows the differences between these two condensers.

No attempt has been made in Table V-1 to assess the overall weight change between Cu-Ni 70-30 and Ti as condenser materials for the example condenser. This overall weight change must include tube sheets, structural elements, waterbox heads, affiliated piping, foundations, etc. Assessment of these weights is beyond the scope of

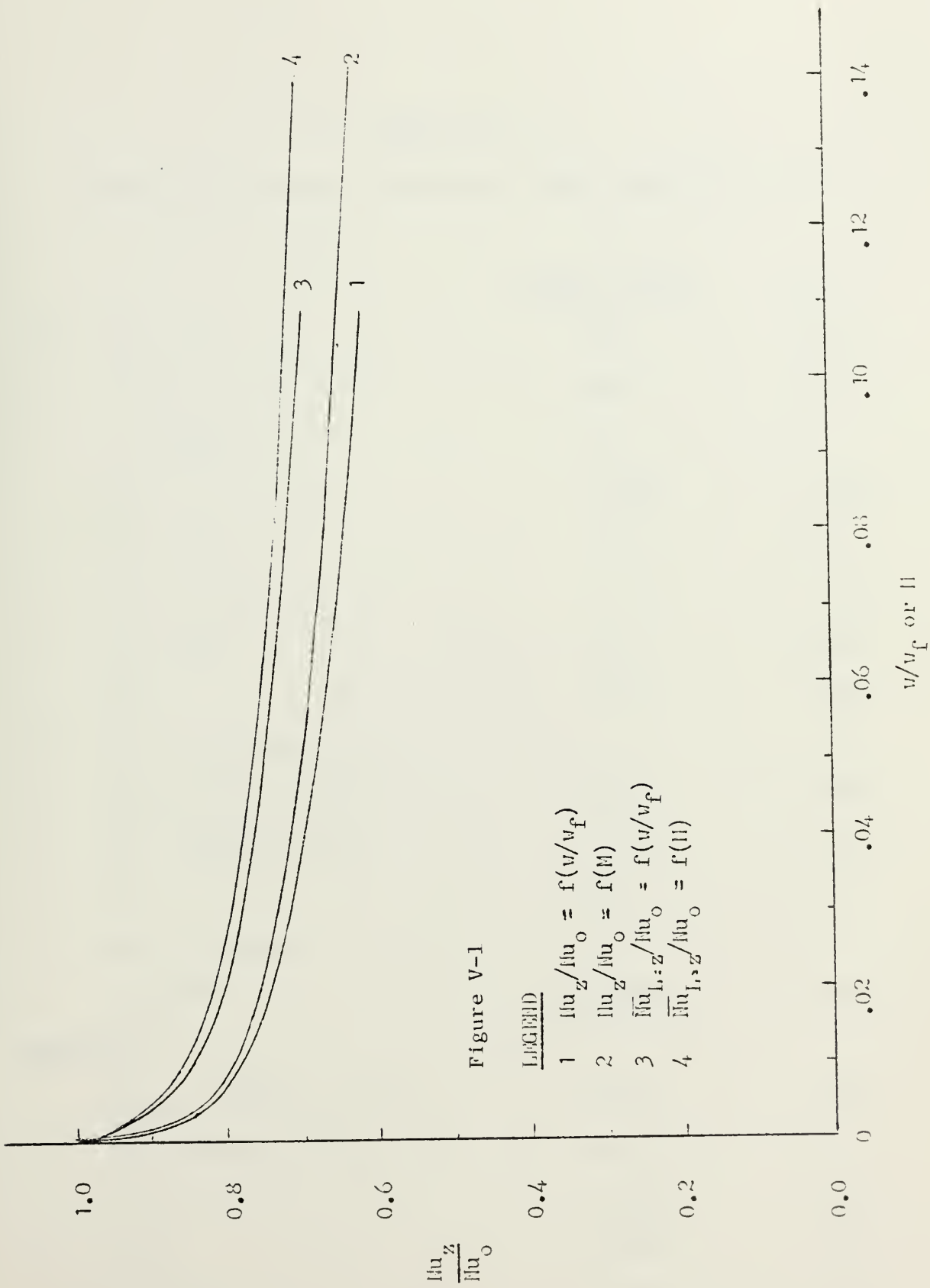


Table V-1

Comparison Between Condensers Using Cu-Ni and Ti

	<u>Cu-Ni 70-30</u>	<u>Ti</u>
D _O (in)	.625	.625
t (in)	.065	.035
a (mils)	18	18
a/p	.13869	.13869
T _{C1} (°F)	65.0	65.0
V _C (ft/sec)	8.0	8.0
W _C (GPM)	7900	8600
N _T	3294	2852
P _C (in-Hg-abs)	5.0	5.0
h _{sc} (BTU/hr ft ² °F)	2000	2000
K (BTU/hr ft°F)	17.0	11.4
F	16	16
No. of passes	2	2
Nu _O ^{1/4}	4.305	4.305

Section 1

h _{cond} (BTU/hr ft ² °F)	12312	11855
U _n (BTU/hr ft ² °F)	487.7	535.7
ΔT (°F)	2.489	2.895
w/w _f	0.060	0.060
L (ft)	4.957	4.426

Table V-1 (Continued)

	<u>Cu-Ni 70-30</u>	<u>Ti</u>
q/A_n (BTU/hr ft^2)	30649	34325
Tc_2	76.36	74.03
<u>Section 2</u>		
\bar{h}_{cond} (BTU/hr $ft^2 \cdot ^\circ F$)	13197	12506
U_n (BTU/hr $ft^2 \cdot ^\circ F$)	501.3	547.9
ΔT ($^\circ F$)	1.988	2.435
w/w_f	0.051	0.053
L (ft)	4.957	4.426
q/A_n (BTU/hr ft^2)	26230	30451
Tc_2 ($^\circ F$)	86.08	82.05
<u>Section 3</u>		
\bar{h}_{cond} (BTU/hr $ft^2 \cdot ^\circ F$)	15302	13628
U_n (BTU/hr $ft^2 \cdot ^\circ F$)	510.8	557.6
ΔT ($^\circ F$)	1.528	2.007
w/w_f	0.019	0.034
L (ft)	2.086	3.148
q/A_n (BTU/hr ft^2)	23383	27351
Tc_2 ($^\circ F$)	89.72	87.16
<u>Section 4</u>		
\bar{h}_{cond} (BTU/hr $ft^2 \cdot ^\circ F$)	15800	14205
U_n (BTU/hr $ft^2 \cdot ^\circ F$)	514.9	564.2
ΔT ($^\circ F$)	1.377	1.754
w/w_f	0.018	0.031

Table V-I (Continued)

	<u>Cu-Ni 70-30</u>	<u>Ti</u>
L (ft)	2.086	3.148
q/A _n (BTU/hr ft ²)	21759	24919
T _{c2} (°F)	93.12	91.83
<u>Section 5</u>		
h _{cond} (BTU/nu ft ² °F)	15178	14405
U _n (BTU/hr ft ² °F)	519.0	569.9
ΔT (°F)	1.262	1.539
w/w _f	0.038	0.039
L (ft)	4.957	4.426
q/A _n (BTU/hr ft ²)	19160	22166
T _{c2} (°F)	100.22	97.66
<u>Section 6</u>		
h _{cond} (BTU/hr ft ² °F)	16441	15326
U _n (BTU/hr ft ² °F)	525.9	576.7
ΔT (°F)	0.974	1.258
w/w _f	0.031	0.034
L (ft)	4.957	4.426
q/A _n (BTU/ft ²)	16011	19287
T _{c2} (°F)	106.15	102.7
q _{total} (BTU/hr)	1.57 x 10 ⁸	1.57 x 10 ⁸
Bundle Diameter (in)	61.8	57.0
Tube Bundle Weight (tons)	10.31	3.78
Weight of Added Water (tons)	--	2.67

this work. Table V-1 shows that a smaller lighter condenser can be designed using Ti, but the penalty is a requirement for increased coolant flow. Table V-2 is an estimate of a comparable horizontal condenser using Cu-Ni 70-30 and designed to meet the same requirements as the condensers presented in Table V-1.

C. Conclusions

This thesis has presented a design methodology for a fluted condenser. It has shown by example in Table V-2 that a fluted condenser can be designed which is more compact than a horizontal condenser. Overall density of the fluted condenser tube bundle increases, however, due to the tube enhancement. This may be off-set by foundation and structural benefits, but that is not addressed here. With a change in material, Table V-1 shows that both volume and weight can be saved at the cost of increased pumping requirements.

Heat transfer coefficients for condensation are predicted by the method described in Chapter III. For flutes which are of the size 12-24 mils in amplitude, increases in the heat transfer coefficients for condensation are greater than eight times that predicted

Table V-2

Comparison Between a Horizontal and a Fluted Condenser*

	<u>Horizontal</u>	<u>Vertical</u>
D_o (in)	.625	.625
t (in)	.065	.065
a (mils)	-	18
a/p	-	.13869
T_{C1} ($^{\circ}$ F)	65.0	65.0
v_c (ft/sec)	8.0	8.0
w_c (GPM)	7900	7900
No. of passes	2	2
N_T	3294	3294
P_c (in-Hg-abs)	5.0	5.0
h_{sc} (BTU/hr 2 $^{\circ}$ F)	2000	2000
K (BTU/hr ft $^{\circ}$ F)	17.0	17.0
L (ft)	14.85	12.0
\bar{U}_o (BTU/hr ft 2 $^{\circ}$ F)	435.8	538.6 ($\bar{U}_n = 509.3$)
$\bar{\Delta T}$ ($^{\circ}$ F)	12.07	1.639
(\bar{q}/A_o) (BTU/hr ft 2)	19627	24257 ($q/A_n = 22936$)
T_{C2} ($^{\circ}$ F)	106.15	106.15
q_{total}	1.57×10^8	1.57×10^8
Bundle Dia. (in)	53.4	61.8
Bundle Wt (tons)	9.68	10.31

*Material for both is Cu-Ni 70-30

by the Nusselt analysis for horizontal tubes. Stress concentrations may be a concern for submarine use, but by limiting the amplitude-to-pitch ratio, stresses can be kept below an acceptable yield criterion. Great gains in weight and volume savings could be realized with enhancement on the cooling water side of the tube in addition to vertical flutes.

D. Recommendations

Because thermal resistance is treated in series, the gains made on the condensation side of a tube may not be fully realized because of the insensitivity of cooling water flow and resistance due to scaling or fouling.

Further investigation is required to consider the following:

1. Internal enhancement: Tremendous gains may be realized by increasing the heat transfer coefficient of the coolant. An internal fin arrangement could accomplish this. Drawbacks to such arrangements are susceptibility to fouling and tube inspectability.

2. Biofouling: The compactness of a titanium marine condenser, or possibly an aluminum stationary condenser, may be to no avail if they are rapidly blocked or fouled by marine organisms. Active and passive protection systems must be investigated which retard or prevent biofouling, and if these are not feasible, an in-service cleaning method must be considered.
3. Scaling: This allowance is a bona fide guess. With new materials, such as titanium, investigation into scaling allowances and mechanisms would allow a less conservative approach to condenser design.
4. Experimental Data: This is an absolute necessity. None has been provided with this thesis because very little is available in the literature concerning fluted tubes. A criticism of the literature cited is that no common terminology is used, nor is design or zero point data usually provided. Furthermore, most work on fluted tubes has been performed with ammonia and various refrigerants.

E. Summary

A proposal has been made in this thesis to design a lighter more compact marine condenser. Calculations have been presented for selecting different condenser tubes for submarine use. Alternative materials have been considered and a comparison condenser design has been presented. A methodology for calculating the heat transfer coefficient for fluted tubes has been presented, and this is incorporated into the condenser sizing procedure.

APPENDIX A

Condenser Tube Stress Calculations

Nomenclature

a	amplitude of the flute (in)
d	tube diameter (in)
h	design depth (ft)
p	pitch of the flute (in)
P	pressure (psi)
t	tube wall thickness (in)
Y	yield criterion (ksi)
YS	yield stress (ksi)
α	stress intensity factor
σ	stress (ksi)
r	cylindrical coordinates
θ	
z	

Subscripts

i	inner diameter
o	outer diameter
x	extreme diameter

The general equations for stress in a thick walled non-fluted tube are [35]:

$$\sigma_r = \frac{-P_i \left[(d_o/d)^2 - 1 \right] + P_o \left[(d_o/d_i)^2 - (d_o/d)^2 \right]}{(d_o/d_i)^2 - 1} \quad (A.1)$$

$$\sigma_\theta = \frac{P_i \left[(d_o/d)^2 + 1 \right] - P_o \left[(d_o/d_i)^2 + (d_o/d)^2 \right]}{(d_o/d_i)^2 - 1} \quad (A.2)$$

$$\sigma_z = -P_i \quad (\text{this is because the tube sheet distributes external pressure on the ends of the tubes}). \quad (A.3)$$

These stresses are shown in Figure A-1. For a condenser, $P_o \ll P_i$ and equations (A.1) and (A.2) simplify to:

$$\sigma_r = \frac{-P_i \left[(d_o/d)^2 - 1 \right]}{(d_o/d_i)^2 - 1} \quad (A.4)$$

$$\sigma_\theta = \frac{P_i \left[(d_o/d)^2 + 1 \right]}{(d_o/d_i)^2 - 1} \quad (A.5)$$

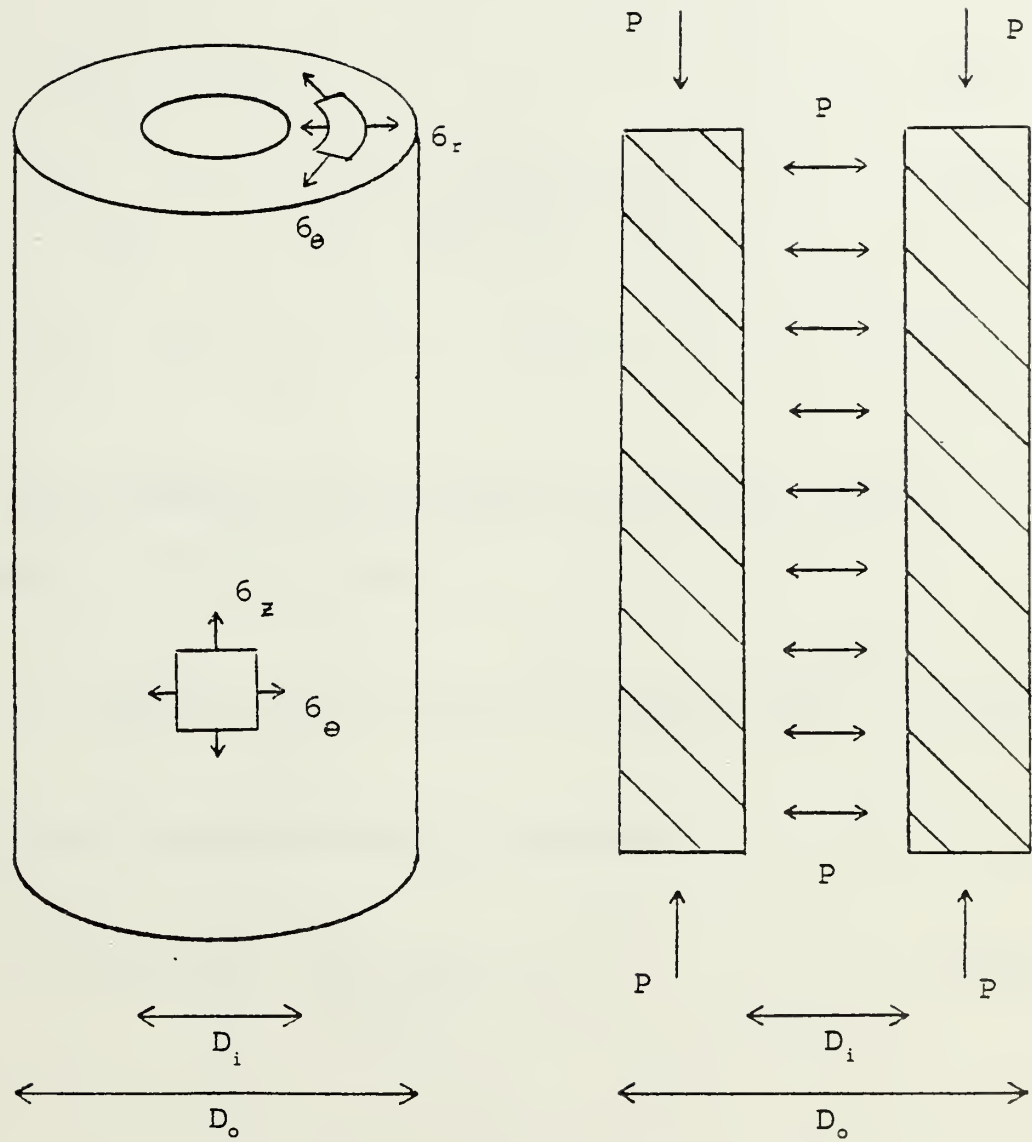


Figure A-1 - Schematic of a condenser tube

Maximum stresses occur at the inner diameter when $d = d_i$

$$\sigma_{r_{\max}} = - P_i \quad (A.6)$$

$$\sigma_{\theta_{\max}} = P_i \left[1 + \frac{2}{(d_o/d_i)^2 - 1} \right] \quad (A.7)$$

$$\sigma_z = - P_i \quad (A.8)$$

The failure criterion used is the Mises yield criterion, γ [35,36] where

$$\gamma = \left\{ \frac{1}{2} \left[(\sigma_r - \sigma_\theta)^2 + (\sigma_\theta - \sigma_z)^2 + (\sigma_z - \sigma_r)^2 \right] \right\}^{1/2} \quad (A.9)$$

For a smooth surface tube this reduces to

$$\gamma = 2 P_i \left[1 + \frac{1}{(d_o/d_i)^2 - 1} \right] \quad (A.10)$$

or

$$\gamma = P_i + \sigma_{\theta_{\max}}$$

For a fluted tube, a stress concentration occurs at the bottom of the flute valley. The mechanical restriction to selecting a fluted tube geometry is to have maximum stresses in the fluted tube which do not exceed a yield criterion which is no greater than the yield criterion for a smooth tube. Since $\sigma_r = 0$ at the surface of the tube, the Tresca yield criterion is appropriate in the form:

$$\frac{Y}{2} = \frac{\sigma_{\theta, \text{flute}} - \sigma_z}{2} \quad (\text{A.11})$$

or

$$Y = P_i + \sigma_{\theta, \text{flute}}$$

The tangential stress for the flute tube at the bottom of the flute, where $d = d_o$, is

$$\sigma_{\theta} = \frac{a P_i \left[\left(\frac{d_x}{d_o} \right)^2 + 1 \right]}{\left(\frac{d_x}{d_i} \right)^2 - 1} \quad (\text{A.12})$$

$$\text{and } d_x \equiv d_o + 4a \quad (\text{A.13})$$

α is a stress intensity or stress concentration factor. By requiring the yield criterion in equation (A.11) to be less than or equal to the yield criterion in equation A-2, a relationship between maximum stress for the two tubes is

$$\frac{\sigma_{\theta \text{ fluted}}}{\sigma_{\theta \text{ max}}} \leq 1 \quad (\text{A.14})$$

For a given fluted tube, compared to a smooth tube of the same inner and outer diameters, a maximum value for α can be determined. Neuber [37] shows a method to relate the amplitude-to-pitch ratio, a/p , with the stress intensity factor. Thus a maximum value for a/p can be determined. This concentration factor for a sine flute can be shown to be

$$\alpha = 1 + \sqrt{\frac{\gamma 2a}{r_o}} \quad (\text{A.15})$$

and

$$r_o = \frac{a}{(2\pi a/p)^2} \quad (\text{A.16})$$

Therefore,

$$\alpha = 1 + \frac{a}{p} 2\pi \sqrt{2\gamma} \quad (\text{A.17})$$

γ is the load relieving factor which is described in reference [37] and accounts for the presence of many flutes on the surface of the tube. It is presented in Figure (A-2).

Y can be related to some mechanical property of the tube material such as yield stress or fatigue limit. For a submarine, a very conservative safety factor of 5 can be assumed [38]. Therefore,

$$Y \leq .2YS \quad (A.10)$$

From reference [2]

$$P_i = h/2248 \text{ ksi} \quad (A.19)$$

with h , the design depth in feet.

Then for a smooth tube

$$.2YS = 2 \left(\frac{h}{2248} \right) \left[1 + \frac{1}{(d_o/d_i)^2 - 1} \right] \quad (A.20)$$

and for a fluted tube

$$.2YS = \left(\frac{h}{2248} \right) \left[\frac{\alpha \left\{ (d_x/d_o)^2 + 1 \right\}}{(d_x/d_i)^2 - 1} + 1 \right] \quad (A.21)$$

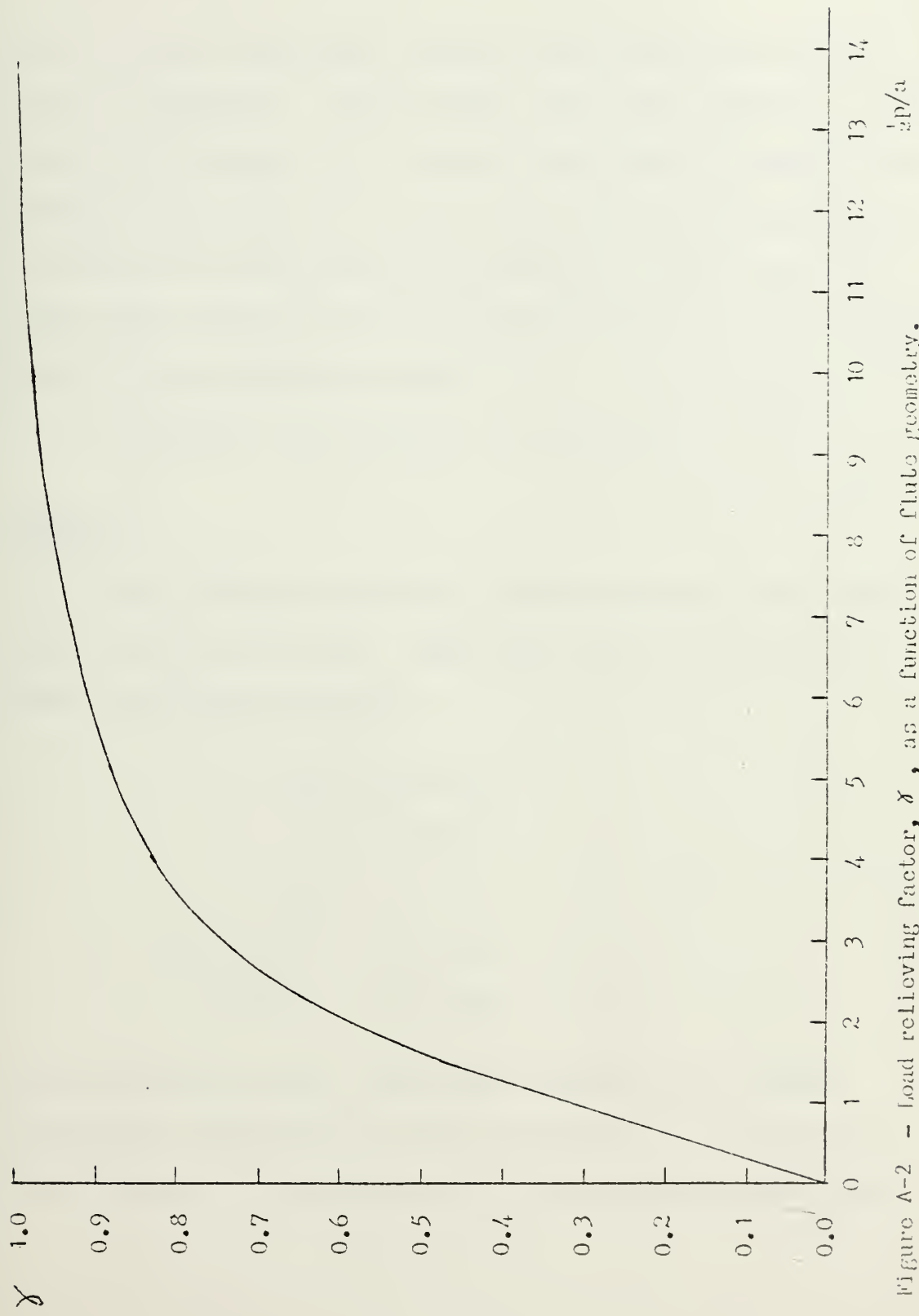


Figure A-2 - Load relieving factor, γ , as a function of flute geometry.

Both of these equations contain the constraints due to material strength, design depth, and tube geometry. The tube wall thickness for a smooth tube can be readily calculated from equation (A.20), and the flute limitations can then be determined from equations (A.19) and (A.17) which will ensure that the yield criterion is not violated due to stress concentrations.

An example calculation is provided.

EXAMPLE

Two different materials are considered for a 2000 ft design depth condenser. These are Cu-Ni 70-30 and Ti. Other specifications are:

$$d_o = .625 \text{ in}$$

$$a = .018 \text{ in}$$

$$d_x = .697 \text{ in}$$

$$YS(\text{Cu-Ni}) = 25 \text{ Ksi}$$

$$YS(\text{Ti}) = 40 \text{ Ksi}$$

From equation (A.20), the inner diameter, d_i , can be calculated and hence the wall thickness, t . Wall thickness, however, is rounded off to the nearest even gauge.

	<u>Cu-Ni</u>	<u>Ti</u>
d_i (in)	.5016	.5511
t (in)	.0617	.0369
d_i (rounded off) (in)	.495	.555
t (rounded off) (in)	.065	.035

Using the rounded values in equation (A.21) to calculate, α , and then using α to determine maximum a/p gives

α	2.0235	2.0559
γ	.82	.81
a/p	.13	.13

In light of the conservative allowance for yield criterion select a/p in both cases as $a/p = .15$.

APPENDIX B

Calculations for Condensate Film Thickness

Nomenclature

a	amplitude of the flute (ft)
A	area (ft^2)
B	dimensional group defined in equation (B.6)
g_c	gravitational constant (lbm ft/lbf hr ²)
h	heat transfer coefficient (BTU/hrft ² °F)
h_{fg}	latent heat (BTU/lbm)
K	thermal conductivity (BTU/hrft°F)
N_u	Nusselt number
p	pitch of the flute (ft)
P	pressure (lbf/ft ²)
q	heat flow (BTU/hr)
r	radius of curvature of the fluted surface (ft)
s_v	flute half perimeter (ft)
s_c	flute arc length on which condensing occurs (ft)
T	temperature (°F)
ΔT	$T_s - T_w$ (°F)
v	velocity (ft/hr)

s }
y } tube surface coordinates
z }

Greek letters

α height of the condensate in the center
of the flute (ft)
 Γ mass flow in S direction per unit length
(lbm/hrft)
 δ condensate film thickness (ft)
 θ angular representation of a point
along the flute surface
 μ dynamic viscosity (lbm/hrft)
 ρ density (lbm/ft³)
 σ surface tension (lbf/ft)
 Φ non-dimensional group defined in eqn (B.12)
 Ω non-dimensional group defined in eqn (B.6)

Subscripts

c coolant
f at flooding conditions
i inside
n nominal
o outside/initial conditions

s saturation

w wall

Symbols

- average

The surface considered is shown in Figure III-2.

The following assumptions are stated explicitly and apply to Figure III-2. [7,9,12,13].

1. The flow of the condensate from peak to valley on the flute surface is thin laminar flow.
2. Because the film is thin, inertia forces are negligible.
3. There is no interfacial shear stress between the liquid and the vapor.
4. There is no flow in the y direction. Flow in the z direction occurs only within the trough of height α .

From a momentum balance on the surface specified,

$$\mu \frac{d^2 v_s}{dy^2} = \frac{dp}{ds} = \frac{d}{ds} \left(\frac{\sigma}{r} \right) \quad (B.1)$$

Integrate this with boundary conditions

$$\frac{dv_s}{dy} = 0 \text{ at } y = \delta$$

and

$$v_s = 0 \text{ at } y = 0$$

The equation for velocity is

$$v_s = \frac{1}{\mu} \frac{dp}{ds} \left(\frac{y^2}{2} - \delta y \right) \quad (B.2a)$$

and

$$\bar{v}_s = \frac{1}{\delta} \int_0^\delta v_s dy = - \frac{1}{\mu} \frac{dp}{ds} \frac{\delta^2}{3} \quad (B.2b)$$

Define the mass flow rate per unit length, Γ .

$$\Gamma = \rho \bar{v}_s \delta = - \frac{\rho}{\mu} \frac{dp}{ds} \frac{\delta^3}{3} \quad (B.3a)$$

and

$$\frac{d\Gamma}{ds} = - \frac{d}{ds} \left[\frac{\rho}{\mu} \frac{dp}{ds} \frac{\delta^3}{3} \right] \quad (B.3b)$$

From an energy balance

$$q/A_s = \frac{K\Delta T}{\delta} = h_{fg} \frac{d\Gamma}{ds} \quad (B.4)$$

Solve eqn (B.4) for $\frac{d\Gamma}{ds}$ and set equal to eqn (B.3b).

$$\frac{K\Delta T}{\rho \sigma h_{fg} g_c} = - \frac{d}{ds} \left[\frac{\rho \sigma}{\mu} \frac{\delta^3}{3} \frac{d}{ds} \left(\frac{\sigma}{r} \right) \right] \quad (B.5a)$$

which, for constant physical properties becomes

$$\frac{\mu K \Delta T}{\rho \sigma h_{fg} g_c} = \frac{\delta}{3} \frac{d}{ds} \left[\delta^3 \frac{d}{ds} \left(\frac{1}{r} \right) \right] \quad (B.5b)$$

Define Ω ,

$$\Omega \equiv \frac{\mu K \Delta T}{\rho \sigma h_{fg} g_c a} = \frac{B \Delta T}{a} \quad (B.6)$$

So eqn. (B.5b) may be written as

$$\Omega = - \frac{\delta}{3a} \frac{d}{ds} \left[\delta^3 \frac{d}{ds} \left(\frac{1}{r} \right) \right] \quad (B.5c)$$

For a sine function flute the radius of curvature, r , is

$$r = \frac{a \left\{ 1 + \left(\frac{2\pi a}{p} \right)^2 \sin^2 \theta \right\}^{3/2}}{\left(\frac{2\pi a}{p} \right)^2 \cos \theta} \quad (B.7)$$

The arc length, S , is

$$S = \int_0^\theta \frac{p}{2\pi} \left\{ 1 + \left(\frac{2\pi a}{p} \right)^2 \sin^2 \phi \right\}^{1/2} d\phi \quad (B.8a)$$

as shown in Figure III-2.

$$\theta_C = \pi \left(1 - \frac{a}{2a} \right) \quad \text{at } s_C \quad (B.8b)$$

For given values of a , p , and Ω , eqn. (B.5c) can be solved numerically [7,12]. By symmetry

$$\frac{d\delta}{ds} = 0 \quad \text{at } \theta = 0$$

Eqn. (B.5c) becomes

$$- \frac{d}{ds} \left[\frac{d}{ds} \left(\frac{1}{r} \right) \right] \Bigg|_{\substack{s=0 \\ \theta=0}} = \frac{3a\Omega}{\delta_0^4} \quad (B.9)$$

which gives the initial value for the boundary layer thickness, δ_0 .

$$\delta_0 = \frac{p}{2\pi} \left[\frac{3\Omega}{1 + 3 \left(\frac{2\pi a}{p} \right)^2} \right]^{1/4} \quad (B.10)$$

Integrating equation (B.5C) gives

$$- \int_{r_0}^{r_s} d\left(\frac{1}{r}\right) = 3a\Omega \int_0^s \frac{1}{\delta^3} \left[\int_0^s \frac{ds}{\delta} \right] ds \quad (B.11)$$

Define ϕ such that

$$\phi \equiv \int \frac{ds}{\delta} \quad (B.12a)$$

and by finite difference

$$\phi_{n+1} = \frac{\Delta s_n}{\delta_n} + \phi_n \quad (B.12b)$$

where

$$\Delta s_n = s_{n+1} - s_n \quad (B.13)$$

Eqn. (B.11) may be written in the form of a trapezoid rule integration to give

$$\frac{1}{r_n} - \frac{1}{r_{n+1}} = \frac{3a\Omega}{\delta_n^3} \left[\phi_{n+1} + \phi_n \right] - \frac{\Delta s_n}{2} \quad (B.14a)$$

which becomes

$$\frac{1}{r_n} - \frac{1}{r_{n+1}} = \frac{3a\Omega}{\delta_n^3} \left[2\phi_n + \frac{\Delta S_n}{\delta_n} \right] - \frac{\Delta S_n}{2} \quad (B.14b)$$

δ_n can now be determined for $\Delta\theta$ increments, with the initial conditions

$$\delta_0 \text{ from eqn (B.10)}$$

$$\phi_0 = 0$$

$$S_0 = 0$$

Addendum 1 to this appendix is a program written for a programmable calculator to solve eqn. (B.14b)

The average film thickness of the condensate can be calculated

$$\frac{1}{\delta} = \frac{1}{S} \int_0^S \frac{dS}{\delta} = \frac{1}{S} \phi(S) \quad (B.15)$$

Define the heat transfer coefficient, h

$$h \equiv \frac{1}{\delta} K \quad (B.16)$$

The average heat transfer coefficient is

$$\bar{h}_s = \frac{1}{\delta} K = K \frac{1}{S_c} \int_0^{S_c} \frac{dS}{\delta} = \frac{K}{S_c} \phi(S_c) \quad (B.17a)$$

where S_c is shown in Figure III-2 and is the arc length over which condensation occurs. By definition

$$\bar{h}_s = \frac{q'}{2S_c \Delta T} \quad (B.17b)$$

where q' is the heat transfer per unit length over the entire flute perimeter. The heat transfer coefficient on the nominal diameter, h_n , may be obtained from the equation for heat transfer

$$q = h A \Delta T \quad (B.18a)$$

From energy conservation,

$$q_s = q_n \quad (B.18b)$$

and therefore

$$\bar{h}_n A_n = \bar{h}_s A_s \quad (B.18c)$$

Then

$$\bar{h}_n = \frac{2S_c}{p} \bar{h}_s = 2K\phi(S_c) \quad (B.19)$$

A Nusselt number may be defined as

$$Nu \equiv \frac{\bar{h}_n p}{K} = 2\phi(S_c) \quad (B.20a)$$

and for $S_c = S_v$

$$Nu = Nu_o(S_v) = 2\phi(S_v) \quad (B.20b)$$

From equations (B.6), (B.8a), (B.8b), and (III-10)

$$\bar{h}_n = f(\Omega, a/p, w/w_f) \quad (B.21)$$

APPENDIX B - ADDENDUM 1

Calculator Program for the
Solution of Equation (B.14b)

This program was written for a Hewlett Packard HP-41C programmable calculator. It requires two additional memory modules, and a printer is highly desireable. Twenty six (26) memories must be allocated. The program is run by simply executing the program label, "DELTA". The calculator will respond by inter-actively asking for inputs. The required inputs are:

a , p , and Ω .

The outputs are for $n = 0$ to $n = 60$,

r_n , s_n , Δs_n , δ_n , and ϕ_n .

The method of solution is exactly as explained in Appendix B. Equation (B.8a) is solved by a 10 point Gauss-Legendre quadrature method for a sine geometry flute.


```
01 LBL "DELTA"
02 "COMPUTER BOUNDARY"
03 "DRY LAYER"
04 AVIEW
05 "AS A FCT. OF AR"
06 "C LENGTH."
07 AVIEW
08 ADV
09 "*****"
10 AVIEW
11 "S<N>/PHI<N>=DEL"
12 "TA<N>,AVG"
13 AVIEW
14 "*****"
15 AVIEW
16 ADV
17 CLRG
18 SCI 4
19 1.488743390 E-1
20 STO 10
21 2.955252247 E-1
22 STO 11
23 4.333953941 E-1
24 STO 12
25 2.692667193 E-1
26 STO 13
27 6.794095683 E-1
28 STO 14
29 2.190863625 E-1
30 STO 15
31 8.650633667 E-1
32 STO 16
33 1.494513492 E-1
34 STO 17
35 9.739065285 E-1
36 STO 18
37 6.667134431 E-2
38 STO 19
39 GTO 10
```

Clear all memories

{

Loading into memory
locations weighting
values necessary for
integration by
quadrature


```

40  LBL 11
41  "INTEGRATION"
42  STO 21
43  X<>Y
44  STO 22
45  -
46  2
47  /
48  STO 22
49  RCL 22
50  RCL 21
51  +
52  2
53  /
54  STO 21
55  0
56  STO 00
57  10.021
58  STO 25
59  XEQ 12
60  XEQ 12
61  XEQ 12
62  XEQ 12
63  XEQ 12
64  RCL 00
65  RCL 20
66  *
67  RTN
68  LBL 12
69  "QUADRATURE SUB-"
70  "ROUTINE"
71  RCL IND 25
72  ISG 25
73  STO 22
74  CHS
75  RCL 20
76  *
77  RCL 21
78  +
79  XEQ 14
80  RCL IND 25
81  *
82  ST+ 00
83  RCL 22
84  RCL 20
85  *
86  RCL 21
87  +
88  XEQ 14
89  RCL IND 25
90  *
91  ST+ 00
92  ISG 25
93  RTN

```

Integration by Gauss-
Legendre Quadrature

$$\int_a^b f(x) dx =$$

$$\frac{b-a}{2} \sum_{i=1}^{10} w_i f \left(\frac{z_i(b-a) + b+a}{2} \right)$$

94 LBL 14
95 "INTEGRAND"
96 SIN
97 RCL 23
98 *
99 2
100 *
101 PI
102 *
103 RCL 24
104 /
105 X^2
106 1
107 +
108 SQRT
109 RCL 24
110 *
111 2
112 /
113 PI
114 /
115 RTN

Integrand:

$$\frac{\sigma}{2\pi} \left\{ 1 + \left(\frac{2\pi a}{p} \right)^2 \sin^2 \theta \right\}^{1/2}$$

116 LBL 10
117 "INITIALIZATION"
118 "ROUTINE"
119 RAD
120 "A<FT>?"
121 PROMPT
122 STO 23
123 " F<FT>?"
124 PROMPT
125 STO 24
126 "OMEGA?"
127 PROMPT

Data input: a, p, Ω

128 3 Calculation of initial
129 * values (continued)
130 RCL 23
131 *
132 STO 09
133 PI $\Delta\theta = \pi/60$
134 60
135 /
136 STO 08
137 0
138 STO 02
139 STO 05
140 STO 06
141 STO 26
142 RCL 23
143 RCL 24 r_o from equation (B.7),
144 /
145 2 $\theta = 0$
146 *
174 PI $s_o = 0$
148 *
149 X² $\phi_o = 0$
150 1/X
151 RCL 23
152 *
153 STO 04
154 "RO<FT>="
155 ARCL X
156 AVIEW
157 0
158 "SO<FT>="
159 ARCL X
160 AVIEW
161 FIX 3
162 "PHIO="
163 ARCL X
164 AVIEW

165 RCL 23 Calculation of initial
166 RCL 24 values (continued)
167 /
168 2
169 *
170 PI
171 *
172 X[↑]2
173 3
174 *
175 1
176 +
177 RCL 23
178 *
179 1/X
180 RCL 09
181 *
182 SQRT
183 SQRT
184 RCL 24
185 *
186 2
187 /
188 PI
189 /
190 STO 03
191 SCI 4
192 "DELTAO<FT>=" δ₀ from equation (B.10)
193 ARCL X
194 AVIEW
195 2
196 STO 25
197 SF 01


```

198 LBL 01           Solution to equation (B.14b)
199 ADV
200 DSE 25
201 RCL 25
202 STO 07
203 1
204 -
205 SF 12
206 FIX 0
207 "N="
208 ARCL X           n
209 AVIEW
210 CF 12
211 SCI 4
212 XEQ 03           Subroutine for equation (B.7)
213 STO 26
214 STO 04
215 "R<N> <FT>=" rn from equation (B.7)
216 ARCL X
217 AVIEW
218 RCL 26
219 RCL 04
220 X<>Y
221 STO 04
222 1/X
223 CHS
224 X<>Y
225 1/X
226 +
227 STO 01
228 0
229 ENTER↑
230 RCL 07
231 ENTER↑
232 RCL 25
233 STO 07
234 RDN
235 XEQ 11           Integration subroutine
236 STO 27
237 RCL 05
238 "S<N><FT>="   Sn = ∫0nΔθ f(θ) dθ   from equa-
239 ARCL X
240 AVIEW
241 RCL 27
242 RCL 05
243 X<>Y
244 STO 05
245 -
246 CHS
247 "DEL,S<N> <FT>=" ΔSn from equation (B.13)
248 ARCL X
249 AVIEW

```


250 STO 06
251 RCL 07
252 STO 25
253 RCL 03
254 STO 07
255 SCI 4
256 FC?C 01
257 XEQ 02 Subroutine to iterate for
258 "DELTA<N> <FT>=" δ_n from equation (B.14b)
259 ARCL X
260 AVIEW
261 RCL 06
262 RCL 07
263 /
264 RCL 02 ϕ_n from equation (B.12b)
265 FIX 3
266 "PHI<N>="
267 ARCL X
268 AVIEW
269 +
270 STO 02
271 2
272 ST+ 25
273 RCL 25
274 63
275 X=Y?
276 GTO 05
277 GTO 81

278 LBL 02
 279 RCL 03 Subroutine to iterate for
 280 1/X δ_n from equation (B.14b)
 281 RCL 06
 282 *
 283 RCL 02 $|\delta_i - \delta_{i+1}| \leq 10^{-7}$
 284 2
 285 *
 286 +
 287 RCL 06
 288 *
 289 2
 290 /
 291 RCL 09
 292 *
 293 RCL 01
 294 X<=0?
 295 GTO 04
 296 /
 297 3
 298 1/X
 299 Y↑X
 300 SCI 4
 301 RCL 03
 302 X<>Y
 303 STO 03
 304 -
 305 ABS
 306 1 E-7
 307 X<=Y?
 308 GTO 02 For $n = 60$, δ_{60} has no
 309 LBL 04 solution. Replace δ_{60} with
 310 RCL 03
 311 RTN δ_{59} .


```

312 LBL 03
313 RCL 08
314 ST* 07
315 RCL 07
316 SIN
317 RCL 23
318 2
319 *
320 PI
321 *
322 RCL 24
323 /
324 STO 01
325 *
326 X↑2
327 1
328 +
329 1.5
330 Y↑X
331 RCL 07
332 COS
333 /
334 RCL 01
335 X↑2
336 /
337 RCL 23
338 *
339 RTN
340 LBL 05
341 BEEP
324 ADV
343 "*****"
344 AVIEW
345 ADV
346 RTN
347 STOP
348 .END.

```


APPENDIX C

Fluted Condenser Sizing Procedure

Nomenclature

a	amplitude of the flute (ft)
A	area (ft^2)
B	dimensional group defined in Appendix B
D	diameter (ft)
F	number of flutes on the tube surface
g_c	gravitational constant (lbm ft/lbf hr^2)
h	heat transfer coefficient ($\text{BTU/hrft}^2 \text{ }^{\circ}\text{F}$)
h_{fg}	latent heat (BTU/lbm)
k	thermal conductivity (BTU/hrft $^{\circ}\text{F}$)
l	ligament (ft)
L	length (ft)
M	non-dimensional group defined in Chapter III
N	number of tubes
Nu	Nusselt number
p	pitch of the flute (ft)
P	pressure (in-Hg-abs)
q	heat flow (BTU/hr)
t	tube wall thickness (ft)
T	temperature ($^{\circ}\text{F}$)
ΔT	$T_s - T_w$ ($^{\circ}\text{F}$)
U	overall heat transfer coefficient ($\text{BTU/hrft}^2 \text{ }^{\circ}\text{F}$)

V	velocity (ft/hr)
w	axial mass flow of liquid (lbm/hr)
wt	weight (lbm or tons)

Greek letters

μ	dynamic viscosity (lbm/hr ft)
ρ	density (lbm/ft ³)
σ	surface tension (lbf/ft)
Ω	non-dimensional group defined in Chapter III

Subscripts

B	tube bundle
C	coolant
D	tube bundle diameter
f	at flooding conditions
i	inside
n	nominal
o	outside
s	saturation
T	total
w	wall
sc	scale
x	cross section

Symbols

-	average
---	---------

This procedure will consist of an example which sizes a submarine condenser. As required in reference [11], a submarine condenser has an even number of passes for the coolant flow. A maximum length will be specified.

Design Specifications

Design depth	= 2000 ft
Material	= Cu-Ni 70-30
Tube:	D_o = 5/8 in (.625 in)
	t = .065 in (16 Gauge)
	a = 18 mils (1.50×10^{-3} ft)
	a/p = .31205
	F = 36
	D_n = .643 in
Coolant:	Sea water
	T_{C1} = 65.0°F
	V_c = 8.0 ft/sec
	w_c = 7900 GPM (4.0559×10^6 lbm/hr)
No. of passes	= 2
No. of passes	= 3294
Condensate:	
Pressure	= 5.0 in-Hg-abs
T_{sat}	= 133.7°F
ρ_{λ}	= 61.554 lbm/ft ³

$$k_x = .376 \text{ BTU/hrft}^{\circ}\text{F}$$

$$\sigma_x = .00459 \text{ lbf/ft}$$

$$h_{fg} = 1017.4 \text{ BTU/lbm}$$

$$\mu_x = 1.20 \text{ lbm/hrft}$$

Thermal conductivity of tube wall = 17.0 BTU/hrft[°]F

$$h_{scale} = 2000 \text{ BTU/hrft}^2{}^{\circ}\text{F}$$

Total tube length per pass = 12.0 ft

Preliminary calculations:

$$Nu_0^{1/4} = 4.612 \text{ from Figure III-4}$$

$$B = 3.7649 \times 10^{-12} \text{ ft/}^{\circ}\text{F} \quad \text{eqn. (III-7)}$$

$$W_f = 6.7157 \text{ lbm/hr} \quad \text{eqn. (III-10)}$$

The condenser will be segmented into 6 sections as shown in Figure (IV-1). The length, L, of section 1 will be that length required for condensate run-off of $w/w_f = 0.060$. This length will be used for sections 2, 5, and 6. The lengths for sections 3 and 4 will be the length necessary to make each pass total length equal to 12.0 ft.

A. Calculation of L_1

1. Specify w/w_f

then $M = .0820$ from equation (III-19)

2. Assume $Tc_2 = 66^{\circ}\text{F}$; $i = 1$

3. Assume $L = 10.0$ ft; $i = 1$

- a. Solve for T_i from equation (III-29)

- b. Solve for $(q/A_n)_i$ from equation (III-25)

- c. Solve for L_{i+1} from equation (III-23)

- d. Repeat a, b, and c until $L_i = L_{i+1}$

4. Solve for Tc_{2j+1} from equation (III-24)

5. Repeat 3 and 4 until $Tc_{2j} = Tc_{2j+1}$

Results are shown in Table C-1.

B. Calculation of $(w/w_f)_2$

1. Specify $L_2 = L_1 = 4.957$ ft.

2. Assume $Tc_2 = 77.36^{\circ}\text{F}$; $j = 1$

3. Assume $\Delta T = 0.50^{\circ}\text{F}$; $i = 1$

- a. Solve for $(q/A_n)_i$ from equation (III-25)

- b. Solve for $(w/w_f)_i$ from equation (III-23)

- c. Solve for M from equation (III-19)

- d. Solve for ΔT_{i+1} from equation (III-29)

- e. Repeat a-d until $\Delta T_i = \Delta T_{i+1}$

TABLE C-1

Solution for L_1 with $(w/w_f)_1 = 0.060$

j	$T_{C_{2j}}$ (°F)	i	L_i (ft)	ΔT_i (°F)	$(q/A_n)_i$ (BTU/hr)	L_{i+1} (ft)	$T_{C_{2j+1}}$ (°F)
1	66.0	1	10.0	.976	33681	4.510	
		2	4.510	2.823	32756	4.638	
		3	4.638	2.720	32807	4.631	
		4	4.631	2.725	32804	4.631	76.36
2	76.36	1	10.0	.976	31419	4.835	
		2	4.835	2.573	30606	4.963	
		3	4.963	2.484	30651	4.956	
		4	4.956	2.489	30649	4.957	76.36
Results:				$(w/w_f)_1 = 0.060$			
				$L_1 = 4.957$ ft			
				$\Delta T_1 = 2.489$ °F			
				$(q/A_n)_1 = 30649$ BTU/hr ft ²			
				$T_{C_2} = 76.36$ °F			

4. Solve for T_{c2j+1} from equation (III-22)

5. Repeat 3 and 4 until $T_{c2j} = T_{c2j+1}$

Results are shown in Table C-2.

Calculation of all remaining length sections proceeds as for section 2, with the desired length specified. The coolant exit temperature for each section is the inlet temperature for the succeeding section.

Results for the entire condenser are shown in Table C-3.

A check on the solution to equation (III-22) verify the results in Table C-3.

$$\bar{h} = .6027 \left(\frac{h_f g_w f}{L \Delta T} \right)^{.0774} \frac{a^{.2307} [f(a/p)]}{p}^{.9226} \left[\frac{K^3 \rho c h_f g_w c}{\mu \Delta T} \right]^{.2307} \quad (III-22)$$

$$\text{where } f[a/p] = \text{Nu}_\infty^{1/4}$$

This should be compared to

$$\frac{(q/A_n)}{\Delta T} = \bar{h} \text{ shown in Table C-3.}$$

Table C-4 shows this comparison.

TABLE C-2

solution for $(w/w_f)_2$ with $L_2 = L_1 = 4.957$ ft

j	$T_{C_{2j}}$	i	ΔT_i (°F)	$(q/A_n)_i$ (BTU/hr)	$(w/w_f)_i$ (°F)	T_{i+1} (°F)	$T_{C_{2j+1}}$ (°F)
1	77.36	1	0.50	29056	.057	2.304	
		2	2.304	28126	.055	2.198	
		3	2.198	28181	.055	2.205	
		4	2.205	28177	.055	2.204	86.80
2	86.80	1	0.50	26828	.053	2.053	
		2	2.053	26015	.051	1.964	
		3	1.964	26062	.051	1.969	
		4	1.969	26059	.051	1.969	86.01
3	86.01	1	0.50	27026	.053	2.075	
		2	2.075	26203	.051	1.985	
		3	1.985	26250	.051	1.990	
		4	1.990	26247	.051	1.989	
4	86.08	1	0.50	27008	.053	2.073	
		2	2.073	26186	.051	1.983	
		3	1.983	26233	.051	1.988	
		4	1.988	26230	.051	1.988	86.08

Results: $(w/w_f)_2 = .051$ $\Delta T_2 = 1.988$ °F $T_{C_2} = 86.08$ °F

$$L_2 = 4.957 \text{ ft} \quad (q/A_n)_2 = 26230 \text{ BTU/hr ft}^2$$

TABLE C-3

Results for Sizing the Condenser Specified

Section	1	2	3	4	5	6
h_c (BTU/hr ft ² °F)	1603	1706	1766	1798	1843	1896
U_w (BTU/hr ft ² °F)	507.8	521.1	528.4	532.3	537.4	543.3
\bar{h} condensing (BTU/hr ft ² °F)	12312	13197	15302	15800	15178	16441
U_n (BTU/hr ft ² °F)	487.7	501.3	510.8	514.9	519.0	525.9
T (°F)	2.489	1.988	1.528	1.377	1.262	0.974
w/w_f	0.060	0.051	0.019	0.018	0.038	0.301
L (ft)	4.957	4.957	2.086	2.086	4.957	4.957
q/A_n (BTU/hr ft ²)	30649	26230	23383	21759	19160	16011
T_{C1} (°F)	65.0	76.36	86.08	89.72	93.12	100.22
T_{C2} (°F)	76.36	86.08	89.72	93.12	100.22	106.15

$$q_{\text{total}} = 1.57 \times 10^8 \text{ BTU/hr}$$

TABLE C-4
Comparison Between Equation (III-22)
and Calculated Results

<u>Section</u>	<u>\bar{h}_n by eqn (22)</u>	<u>\bar{h}_n by iterative solution</u>
1	12322	12312
2	13206	13197
3	15313	15302
4	15812	15800
5	15190	15178
6	16452	16441

C. Sizing the Tube Bundle Diameter

The number of tubes across the diameter, N_D , of a circular bundle containing N_T total number of tubes is

$$N_D = \sqrt{\frac{4N_T}{\pi}} \quad (C.1)$$

The geometric diameter for the individual tube used in sizing the tube bundle is the extreme diameter, D_x

$$D_x = D_o + 4a \quad (C.2)$$

The physical separation in the tube sheet between outer edges of adjacent tubes is termed the ligament, l . Minimum ligament distance is 0.212 in. [42]. This limit is set by manufacturing constraints. Thus the tube bundle diameter, D_B , is

$$D_B = N_D \cdot D_x + (N_D - 1) \cdot l \quad (C.3)$$

For the condenser considered,

$$N_D = 65$$

$$D_x = .6970 \text{ in.}$$

$$D_B = 58.87 \text{ in.}$$

Allowing 5 percent for steam flow passages, structural members, air ejectors, and downcomers gives an external diameter for the condenser bundle

$$D_B = 61.82 \text{ in.}$$

D. Weight Estimation of the Tube Bundle

The weight of an individual tube can be determined by the product of the tube length, L , tube cross section, A_x , and material density. Thus the weight of the tube bundle is

$$Wt_B = A_x L \rho N_T \quad (C.4)$$

The cross sectional area for a sine geometry flute is approximated by

$$A_x = \frac{(D_n^2 - D_i^2)}{4} \quad (C.5)$$

For the condenser considered,

$$A_x = .1507 \text{ in}^2$$

$$Wt_B = 23091 = 10.31 \text{ tons}$$

REFERENCES

1. Taggart, R., Ed., Ship Design and Construction, Society of Naval Architects and Marine Engineers, New York, 1980.
2. Jackson, H., "Submarine Design Notes", Dept. XIII-A Professional Summer at MIT, 1980.
3. Lecture by Mr. Dan Weiler of Naval Sea Systems Command, 3211, to MIT XIII-A students on 8 January 1980.
4. "Shaping the General Purpose Navy of the Eighties: Issues for Fiscal Years 1980-1985", Congressional Budget Office, Congress of the United States, January 1980.
5. Couhat, J., Combat Fleets of the World, 1981/81, United States Naval Institute, Annapolis, MD, 1980.
6. Rohsenow, W. and Choi, H., Heat, Mass and Momentum Transfer, Prentice-Hall, Englewood Cliffs, NJ, 1961.
7. Gregorig, R., "Hautkondensation an feingewellten Oberflächen bei Berücksichtigung der Oberflächen- spannung," Zeitschrift für angewandte Mathematik und Physik, Vol. 5., 1954, pp. 36-49.
8. Zener, C. and Levi, A., "Drainage Systems for Condensation," Journal of Engineering for Power, Vol. 96, July, 1974, pp. 209-215.
9. Webb, R., "A Generalized Procedure for the Design and Optimization of Fluted Gregorig Condensing Surfaces," Journal of Heat Transfer, Vol. 101, May, 1979, pp. 335-339.
10. Conversation with Professor B. Mikic, MIT on 26 February 1981.
11. Military Specification, "Condensers, Steam, Naval Shipboard," MIL-C-15430J (Ships), 19 June 1974.
12. Yamamoto, H. and Ishibachi, T., "Calculation of Condensation Heat Transfer Coefficients of Fluted Tubes," Heat Transfer Japanese Research, Vol. 6., October - December, 1977, pp. 61-68.

13. Panchal, C. and Bell, K., "Analysis of Nusselt-Type Condensation on a Vertical Fluted Surface," Condensation Heat Transfer, ASME, New York, 1979, pp. 45-54.
14. Mori, Y., Hyikata, K., Hirasawa, S., and Nakayama, W., "Optimized Performance of Condensers with Outside Condensing Surface," Condensation Heat Transfer, ASME, New York, 1979, pp. 55-62.
15. Krassik, I., Krutzsch, W., Fraser, W., and Messina, J., eds., Pump Handbook, McGraw-Hill, New York, 1976.
16. Harrington, R., ed., Marine Engineering, SNAME, New York, 1971.
17. Letter from Commander, David W. Taylor Naval Ship Research and Development Center to Commander, Naval Sea Systems Command (SEA 05DC3), Ser 10310, dated 7 January 1980.
18. Metals Handbook, Ninth Edition, Vols. 2 and 3, American Society for Metals, Metals Park, OH, 1979.
19. Efird, K., and Anderson, D., "Sea Water Corrosion of 90-10 and 70-30 Cu-Ni: 14 Year Exposures," Materials Performance, Vol. 14, November, 1975, pp. 37-40.
20. Bulow, C., "Use of Copper Base Alloys in Marine Services," Naval Engineers Journal, Vol. 77, June 1965, pp. 470-482.
21. Danek, G., "The Effect of Sea Water Velocity on the Corrosion Behavior of Metals," Naval Engineers Journal, Vol. 78, October, 1966, pp. 763-769.
22. Fontana, M. and Greene, N., Corrosion Engineering, 2d ed., McGraw-Hill, New York, 1978.
23. Litvin, D., and Smith, D., "Titanium for Marine Applications," Naval Engineers Journal, Vol. 83, October, 1971, pp. 37-43.
24. Knudsen, J., "Apparatus and Techniques for Measurement of Fouling of Heat Transfer Surfaces," Condenser Biofouling Control, Symposium Proceedings, Electric Power Research Institute, Ann Arbor Science Publishers, Ann Arbor, MI 1980.

25. Characklis, W., Bryers, J., Trulear, M. and Zelver, N., "Biofouling Film Development and Its Effects on Energy Losses: A Laboratory Study," Condenser Biofouling Control, Symposium Proceedings, Electric Power Research Institute, Ann Arbor Science Publishers, Ann Arbor, MI, 1980.
26. Letter from Commander, David W. Taylor Naval Ship Research and Development Center to Commander, Naval Sea Systems Command (SEA 532), Ser 2722, dated 23 July 1980.
27. Bell, K., "The Effect of Fouling on OTEC Heat Exchanger Design, Construction, and Operation," Unpublished, received by private communication, September 1980.
28. Blume, W. and Kirk, B., "Application of the Cathelco Antifouling System for the Control of Marine Growth in Seawater Inlets and Condensers," Condenser Biofouling Control, Symposium Proceedings, Electric Power Research Institute, Ann Arbor Science Publishers, Ann Arbor, MI, 1980.
29. Conversation with Mr. Alan Fritsch, David W. Taylor Naval Ship Research Development Center, Annapolis, Maryland, on 14 June 1980.
30. Brown, B., et al, Marine Corrosion Studies, NRL Memorandum 1574, Second Interim Report of Progress, U.S. Naval Research Lab, Washington, DC, November, 1964.
31. Uhlig, H., Corrosion and Corrosion Control, 2d ed. John Wiley and Sons, New York, 1971.
32. Cotton, J. and Downing, B., "Resistance of Titanium to Sea Water," Transactions of the Institute of Marine Engineers, Vol. 69, August, 1957, pp. 311-319.
33. LaQue, F., "Deterioration of Metals in an Ocean Environment," Ocean Engineering, Vol. 1, March, 1969, pp. 299-312.
34. Conversation with Mr. Kurt Bredehorst and Mr. Walter Aerni of NAVSEA on 15 June 1980.

35. Crandall, S., Dahl, N. and Lardner, T., eds., An Introduction to the Mechanics of Solids, 2d ed., McGraw-Hill, New York, 1972.
36. McClintock, F. and Argon, A., eds., Mechanical Behavior of Materials, Addison-Wesley, Reading, Massachusetts, 1966.
37. Neuber, H., Theory of Notch Stresses, Principles for Exact Stress Calculation, J. W. Edwards, Ann Arbor, Michigan, 1946.
38. Conversation with CAPT Harry A. Jackson, USN (Ret.) on 18 November 1980.
39. Welty, J., Engineering Heat Transfer, John Wiley and Sons, New York, 1978.
40. Fugii, T. and Honda, H., "Laminar Filmwise Condensation on a Vertical Single Fluted Plate," Sixth International Heat Transfer Conference, Vol. 2, National Research Council of Canada, Toronto, Canada, August 7-11, 1978, pp. 419-424.
41. Harrington, R., ed., Marine Engineering, Society of Naval Architects and Marine Engineers, New York, 1971.
42. Conversation with Mr. Henry Brawn of DeLeval Corp., Florence, NJ, on 12 August 1980.
43. Titus, M., "Investigation of Rolled Titanium Tube-To-Tube Sheet Joints for Condenser Application," David W. Taylor Naval Ship Research and Development Center, Bethesda, MD, October, 1978.

Thesis

B2293

Barnes

c.1

Marine surface con-
denser design using
vertical tubes which
are enhanced.

202534

Thesis
B2293 Barnes 202564
c.1
Marine surface con-
denser design using
vertical tubes which
are enhanced.

thesB2293

Marine surface condenser design using ve



3 2768 002 01426 8

DUDLEY KNOX LIBRARY